A novel classification of planar four-bar linkages and its application to the mechanical analysis of animal systems

M. MULLER

Department of Experimental Animal Morphology and Cell Biology, Agricultural University, Marijkeweg 40, 6709 PG Wageningen, The Netherlands

CONTENTS

SUMMARY

A novel classification of planar four-bar linkages is presented based on the systematical variation of one, two or three bar lengths and studying the transmission properties (input-output curves) of the linkages. This classification is better suited to the study of biological systems than the classical Grashof-classification used in engineering as it considers the change of structural elements, in evolution for example, instead of evaluating the possibilities for the rotation of a particular bar.

The mechanical features of a wide range of planar linkages in vertebrates, described by various authors, have been included in this classification. Examples are: skull-levation and jaw-protrusion mechanisms in fishes, reptiles and birds, the coral crushing apparatus of parrotfishes, and catapult-mechanisms in feeding pipefishes. Four-bar replacement mechanisms, e.g. crank-slider mechanisms in feeding systems of fishes and cam-mechanisms in mammalian limb-joints, and more complex linkages than four-bar ones, e.g. six-bar linkages and interconnected four-bar linkages in fish feeding mechanisms, are also discussed.

In this way, an overview is obtained of the applicability of planar linkage theory in animal mechanics to mechanical functioning and the effect of possible variations of bar lengths and working ranges in evolution. Four-bar system analysis often provides a rigorous method of simplifying the study of complex biological mechanisms. The acceptable width-range of necessary and undesired hysteresis ('play') in biological linkages is also discussed.

1. INTRODUCTION

In many biological systems, skeletal elements cannot be moved by the muscles directly. For example, in head expansion of fish during feeding, there are no muscles lateral to the head which are strong enough to move the suspensoria (cheeks) and opercula (gill covers) in a lateral direction (abduction). In such cases, these elements have to be moved via a chain of bones and ligaments called a linkage (Alexander 1983). In engineering, linkages are widely applied with an almost infinite variety (see e.g. Hartenberg & Denavit 1964; Dijksman 1976; Hunt 1978; Reuleaux 1983). This 'theory of machinery' has become a separate discipline in mechanics. Its importance is indicated by a literature-'explosion' during the past 50 years.

In biology, several linkages have been described in different animals and for different functions (various authors, see later). However, a comprehensive underlying theory which merges engineering- and biological principles and which gives a systematic overview about the variety of linkages is still lacking. It is the aim of this paper to present such a framework. The advantage of this approach is that the structure and the particular mechanical properties of linkages can be better understood and that it gives insight in possible evolutionary changes in biological linkages.

The linkage with the simplest construction consists of four elements (bars or links) which are movably connected in parallel planes (Hartenberg & Denavit 1964: §2.8). It has a so-called mobility 1 (also denoted as a single degree of freedom in motion) (Dijksman 1976; Alexander 1983), i.e. the movement of a particular element determines the movement of all the other elements. It is already difficult to obtain a complete overview of all possible variations of this so-called planar four-bar linkage.

The main discussion in this article will be concentrated on planar four-bar linkages, with some excursions to more complex systems. In the first part of the paper, a new classification of four-bar linkages, more suitable for biological applications than the current engineering one, will be given. The second part considers examples of different linkages in animals and discusses their mechanical behaviour using the theory presented and developed in the first part.

2. DEFINITIONS

In this section the following definitions and terminology will be stated (for technical background see, for example, Hartenberg & Denavit 1964; Hunt 1978; Dijksman 1976; Reuleaux 1983). Figure 1 gives an arbitrarily chosen example of a four-bar linkage in which the names and abbreviations of bars, joints and angles are defined. These definitions are used consistently in this paper.

1. A four-bar 'linkage' (or '-chain', '-system') is the combination of the bar lengths itself. A 'configuration' is the shape of the linkage for any input angle (see below). A 'position' resembles a fixed configuration of the linkage (i.e. for a particular input angle). A 'crank' (c) is a bar which can make a complete revolution, a 'rocker' (r) can only oscillate. In engineering texts, double crank (cc), crank-rocker (cr or rc) and double rocker (rr) linkages are distinguished (table 1; see also §10 of Dijksman 1976).

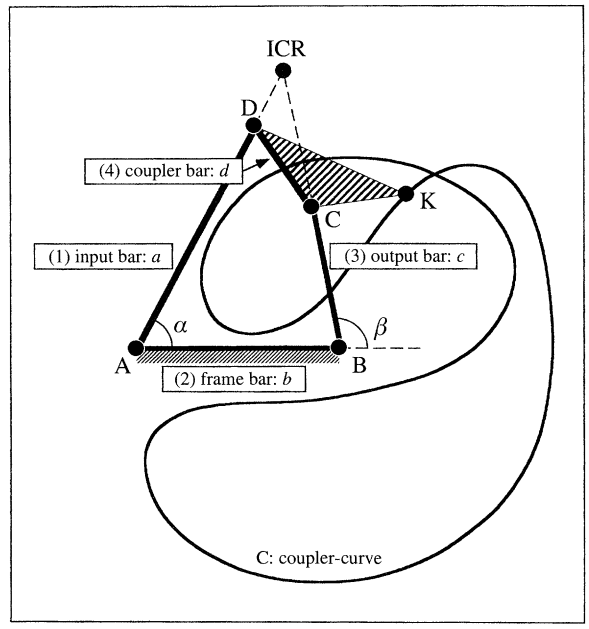

Figure 1. An example of a planar four-bar linkage with angles, joints, points and bars defined. These definitions are consistently used throughout the paper. Modified after Hunt (1978). The bars and joints are always indicated by the same alphabetic characters, numbers and names. α = input angle, β = output angle. Approximate bar lengths are: (a, b, c, d) ≡ (26, 20, 15, 10). The hatched triangular area is a part of the coupler plane. K is an arbitrary point in this plane. Curve C is an example of a coupler plane curve. The instantaneous centre of rotation (ICR) or pole is at the crossing of the continuations of bars a and c. The locus of the pole for all positions of the linkage is called 'polode' or 'centrode'. Two polodes exist: a 'fixed' and a 'moving' one (see text and figure 2b). These curves have a rather complex shape and are therefore not drawn in this figure.

2. The angle α is the 'input angle', the angle β the 'output angle' to be calculated (α and β are mostly considered in the interval [0,360°]). Considering other angles of the linkage as in- and output-variables or considering the linkage with changed bar-lengths is called a 'transformation'. Considering different bars as the frame is called an 'inversion' of the linkage. A plot of β as a function of α is called an 'input-output function' or (kinematic) 'transmission function'. The transmission function has a very characteristic shape, so the type of a four-bar linkage can immediately be read from it. Simple methods to determine β from given bar lengths and α are e.g. described by Elshoud (1986) using intersecting circles and Aerts & Verraes (1984) and Westneat (1990) using the cosine rule. The 'transmission ratio' (transmission-coefficient of Barel *et al.* 1975) is $d\beta/d\alpha$. When the six quantities (a, b, c, d, α and β; see figure 1) are known, any angle between the bars can be easily determined and by this all other properties of the linkage (see below).

3. 'Coupler curves' are trajectories which points of the plane connected to the 'coupler-bar' d (e.g. point K in figure 1) make in the plane of the frame bar b.

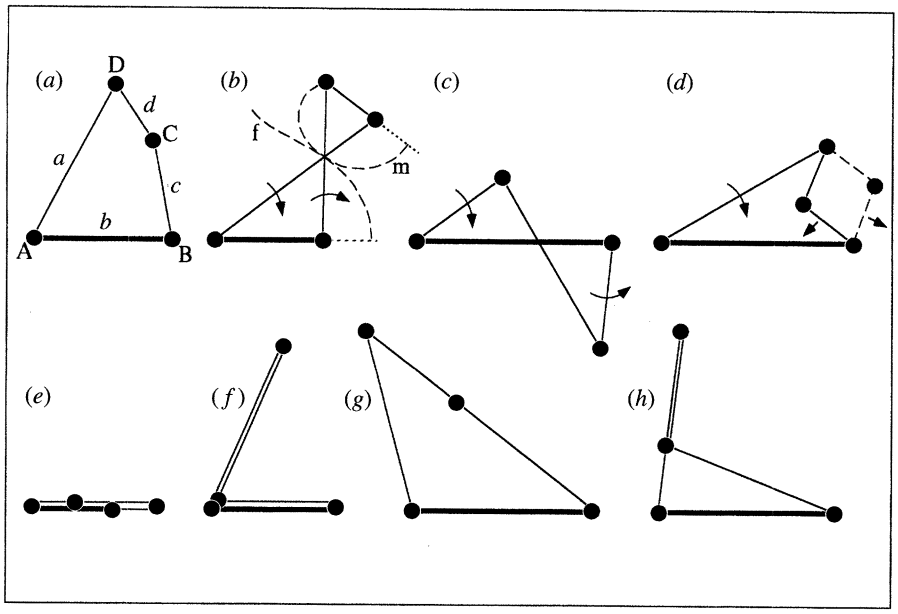

Figure 2. Important positions and configurations of different planar four-bar linkages. Frame bars *b* are drawn bold. (*a*) uncrossed configuration; (*b*) conversely crossed configuration. For this configuration, the fixed (f) and moving (m) polodes are drawn; (*c*) reversely crossed configuration; (*d*) conversely (broken line) and reversely (solid line) folding configurations; (*e*) branched or transition-position; (*f*) undetermined position; (*g*) stretched in-line position of *d* with *c* (uncrossed-uncrossed transition); (*h*) overlapping in-line position (uncrossed-crossed transition).

Table 1. *Engineering classification of planar four-bar linkages (Hartenberg & Denavit 1964: §3.3; Hunt 1978: §3.10; Dijksman 1976: §10)*

(Only in the Grashof-linkages (type 1) and the special transition-linkages (types 3 and 4) the shortest link(s) can make a complete revolution. a = input link, b = frame (or base-) link, c = output link, d = coupler link. s = shortest link, l = longest link, p and q: remaining links. c = crank = revolving bar, r = rocker = oscillating bar, cc = double crank linkage, cr = crank-rocker linkage, rc = rocker-crank linkage, rr = double rocker linkage.)

'if'	'and'	type (Hartenberg & Denavit 1964)	movement class	remarks (Dijksman 1976)
$s+l<p+q$	$s=a$	1a Grashof	cr	– always at least one revolving bar
$s+l<p+q$	$s=c$	1b Grashof	rc	– no image position
$s+l<p+q$	$s=b$	1c Grashof	cc	– incomplete coupler motion
$s+l<p+q$	$s=d$	1d Grashof	rr	– bicursal coupler curves
$s+l>p+q$		2a,b,c,d	rr	– three bars oscillate
$s+l=p+q$	$s=a$	3a	cr	– branching linkages; – shortest bar s can make complete revolution; – image position possible; – complete coupler motion; – unicursal coupler curves
$s+l=p+q$	$s=c$	3b	rc	
$s+l=p+q$	$s=b$	3c	cc	
$s+l=p+q$	$s=d$	3d	rr	
$a=c$	$b=d$	4a Parallellogram	cc	
$a=b$	$c=d$ and $s=b$	4b Kite	cc	– folding system
$a=d$	$c=b$ and $s=b$	4b Kite	cc	
$a=b$	$c=d$ and $l=b$	4c Kite	rc	
$a=d$	$c=b$ and $l=b$	4c Kite	cr	

Sometimes, parts of these curves are virtually straight lines (Dijksman 1976; Badoux 1984).

4. The 'instantaneous centre of rotation' (ICR) can be found at the intersection of the (extensions of the) in- and output-bar. The ICR is also called the '(velocity-) pole' because this point is the only point of the coupler plane having zero (linear) velocity. When infinitesimal quantities are considered, the pole and ICR are identical. For finite displacements, this is not the case. A discussion about poles and ICR's for such displacements can be found in Alexander & Dimery (1985).

The locus of the ICR for all positions of a four-bar linkage is the 'polode' or 'centrode' (figure 1, Dijksman 1976). Two polodes exist: a 'fixed polode', which can be constructed taking the frame bar *b* fixed and plotting the locus of the ICR for different positions of the linkage, and a 'moving polode', taking the the coupler bar *d* fixed (figure 2*b*; for other examples, see e.g. Muller 1993*b*). As at the ICR the

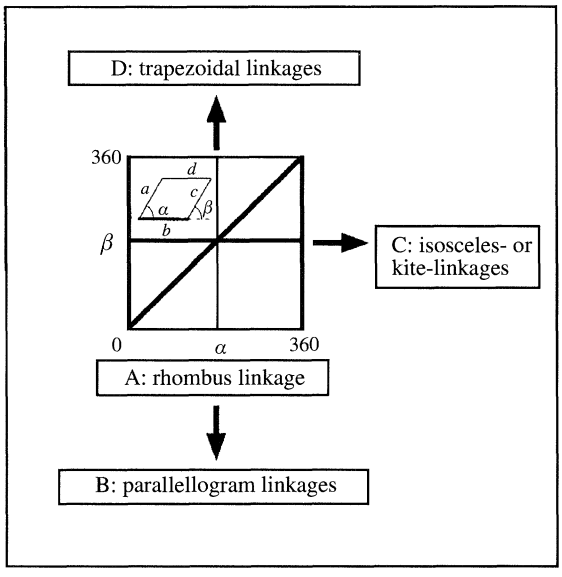

Figure 3. Scheme for parameter classification of four-bar linkages. Starting from a rhomboid linkage (one-parameter linkage), three classes of 2-parameter linkages are derived. The transmission function of a rhombus provides the asyptotes of the transmission functions of 2-parameter linkages. Three asymptotes can be distinguished: (1) the line $\alpha = 0°$ or 360°, (2) the line $\beta = 180°$, (3) the line $\alpha = \beta$. Further explanation in text (§3). For parallellogram linkages see figure 4; for isosceles linkages see figure 5; for trapezoidal linkages see figure 6.

(linear) velocities of both the frame- and the coupler plane are zero, the polodes roll over each other during movement of the linkage, without sliding (Menschik 1974*a*; Alexander & Bennett 1987; Muller 1993*a*, *b*).

In figure 2, all possiblities for special configurations and positions of planar four-bar chains are shown.

A transmission function gives for any α two, one, no or an infinite number of values of β. No values for β exist when the position of the linkage is impossible. Generally, a four-bar linkage can have an 'uncrossed' (figure 2*a*) or 'crossed' (figure 2*b*, *c*) configuration. In a 'conversely' (figure 2*b*) crossed configuration, the in and output bars rotate in the same direction, in a 'reversely' (figure 2*c*) crossed configuration, these bars rotate in opposite directions. Sometimes, crossing is impossible. Then, the linkage can be only conversely (outwards) and reversely (inwards) 'folded' (figure 2*d*). Basically, the movements of four-bar linkages are (highly) non-linear. It has to be considered as a special case when a more or less linear relation between α and β occurs.

Linkages may move through 'branched' (or 'transition-', 'change point-') positions (figure 2*e*), in which they can change from an uncrossed to a crossed situation and vice versa. Then, some bars may change their direction of rotation (Hartenberg & Denavit 1964). Comparable 'branched' positions may also occur between inwards folding and outwards folding configurations (§4*b*). In an 'undetermined position' (figure 2*f*), α and β are independent of each other: at a single α, an infinite amount of values of β is possible or vice versa (figure 3).

Single values for α and β may be obtained when two bars are in a 'stretched in-line' (figure 2*g*) or 'overlapping in-line position' (figure 2*h*). In an 'overlapping in-line' position, the linkage may be 'locked' i.e. fixed to an immobile position (to behave as a rigid unit; see Muller 1987).

When a transmission function consists of two separate parts, the four-bar linkage has to be dismounted to obtain the 'image configurations' of the chain. In these cases, the coupler curves are broken up

Table 2. *Overview of four bar type codes*

(Transmission functions are shown in Figs. 4, 5, 6, 9 and 10. Isosceles linkages are denoted by a 'K' from 'Kite' to avoid confusion with other characters. The type codes for three parameter series in which one of the bars is varied are shown in table 5. For example, the type code 3Pslsl(1) means: a series of three parameter systems, based on the linkage 2Pslsl, in which bar 1 (= bar *a*) is varied. 2- and 3-parameter types which resemble particular four-bar types concerning their transmission functions (approximate function cognates) are placed within quotation marks.)

type code	system description
1R	one parameter (= one bar length) system: rhombus
2Pslsl	two parameter system: parallellogram; bar *a* is short (*s*)
2Plsls	two parameter system: parallellogram; bar *a* is long (*l*)
2Kssll	two parameter system: kite; (*a*,*b*,*c*,*d*) = short-short-long-long
2Kllss	etc.
2Klssl	
2Kslls	
2T1s	two parameter system: trapezoid; bar *a* = bar 1 is short (*s*)
2T1l	two parameter system: trapezoid; bar *a* = bar 1 is long (*l*)
2T2s	two parameter system: trapezoid; bar *b* = bar 2 is short (*s*)
2T2l	etc.
2T3s	
2T3l	
2T4s	
2T4l	
3Sopp(lmsm)	three parameter system: medium bars (*m*) equal and opposite; (*a*,*b*,*c*,*d*) = long-medium-short-medium
3Sadj(lsmm)	three parameter system: medium bars (*m*) equal and adjacent; (*a*,*b*,*c*,*d*) = long-short-medium-medium

in two branches ('incomplete' or 'bicursal'). For continuous transmission functions, all configurations (and so the image configurations) can be obtained leaving the linkage intact. In the latter cases, coupler curves are also continuous ('complete' or 'unicursal').

3. CLASSIFICATIONS

In engineering, classification of planar four-bar linkages is centered about the possibility of an element making a complete revolution. This so-called 'Grashof-classification' (table 1) is very relevant when motors are used to drive the linkages. In biological systems, such continuously rotating elements are absent and so the Grashof-classification is less relevant. Instead, the possibility of changes in the size and shape of elements and of the working range are important. Therefore, I designed a new theoretical classification of planar four-bar linkages which is better suited for this purpose. This new classification matches the Grashof-one (as it should do!) but considers the properties of four-bar linkages from a different viewpoint.

Regarded formally, a four-bar chain contains four independent parameters i.e. the lengths of the bars a, b, c and d, and a motion variable (α). Transmission functions may be studied for different values of a, b, c and d, but also the 'working range' for α may be varied (shifted and/or extended), implying a five- or more-parameter approach. In some fortunate cases a combination of parameters can be made (e.g. in bilaterally symmetric systems) resulting in a two- or even a one-parameter approach by combining the two parameters (Muller 1987, 1989).

The only one-parameter linkage is the rhombus (1R-linkage: all bars equal: $a = b = c = d$; table 2, figure 3). The rhombus is a double crank linkage showing linear transmission over the entire range [0,360°]: $\beta = \alpha$, except for $\alpha = 0 + k.360°$ where β is undetermined and $\beta = 180 + k.360°$ where α is undetermined. No crossed or folding configurations exist.

Starting from the rhombus, three different types of two-parameter linkages may be derived: 'parallellogram' linkages in which opposite links are equal, 'isosceles-' or 'kite' linkages in which two adjacent links are equal and 'trapezoidal' linkages in which three bars are equal (figure 3). Although the rhombus in itself has no very interesting properties, it is an important linkage because all two- (or more-) parameter transmission curves have the transmission curve of the rhombus as an 'asymptote'. Thus, some sense for the shape of a two-parameter curve can be obtained by, for a moment, adjusting its parameters to give almost a rhombus (see also Fichter & Hunt 1979).

The asymptotic nature of two- or more-parameter transmission curves implies also that they usually show a 'non-linear behaviour'. A particular form of non-linear transmission is found in a 'transient mechanism' in which for a small change of the input angle (α or β) a rather large variation of the output angle results (see, for example, figure 4 and §4*a*).

To provide an easy reference to the various types of

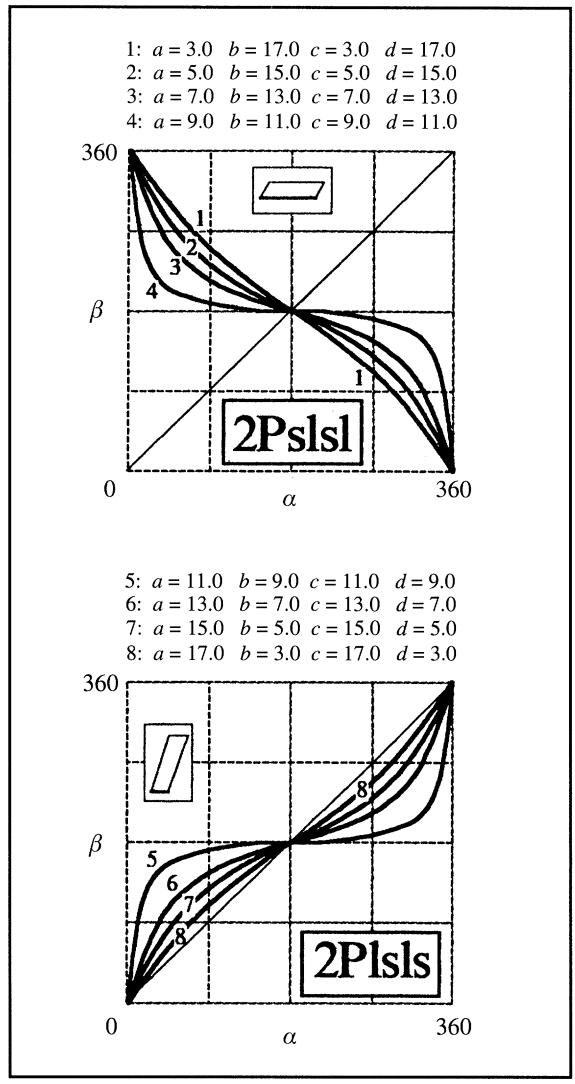

Figure 4. Transmission functions of parallellogram linkages. The perimeter of the different linkages is kept constant. The solid bar in the inset denotes the frame-link b, the left bar is the input-link a. The line $\alpha = \beta$ represents the transmission function for uncrossed configurations, the bold lines give the transmission function for crossed configurations. The codes are defined in table 2. Further explanation in text (§4*a*).

2- and 3-parameter four-bar linkages, I designed a simple 'identification code' (table 2). This code will be used throughout this article. The transmission properties of the four-bar linkages can be read in figures 4, 5, 6, 9 and 10.

4. TWO-PARAMETER LINKAGES

Fourteen different two-parameter linkages can be distinguished, belonging to the classes: parallellogram linkages, isosceles- or kite linkages and trapezoidal linkages altogether already cumulatively giving a great variation in transmission curves. Within one class, the two-parameter system may be reduced to a one-parameter system because the ratio between the parameters then fully defines the linkage (Muller 1987, 1989).

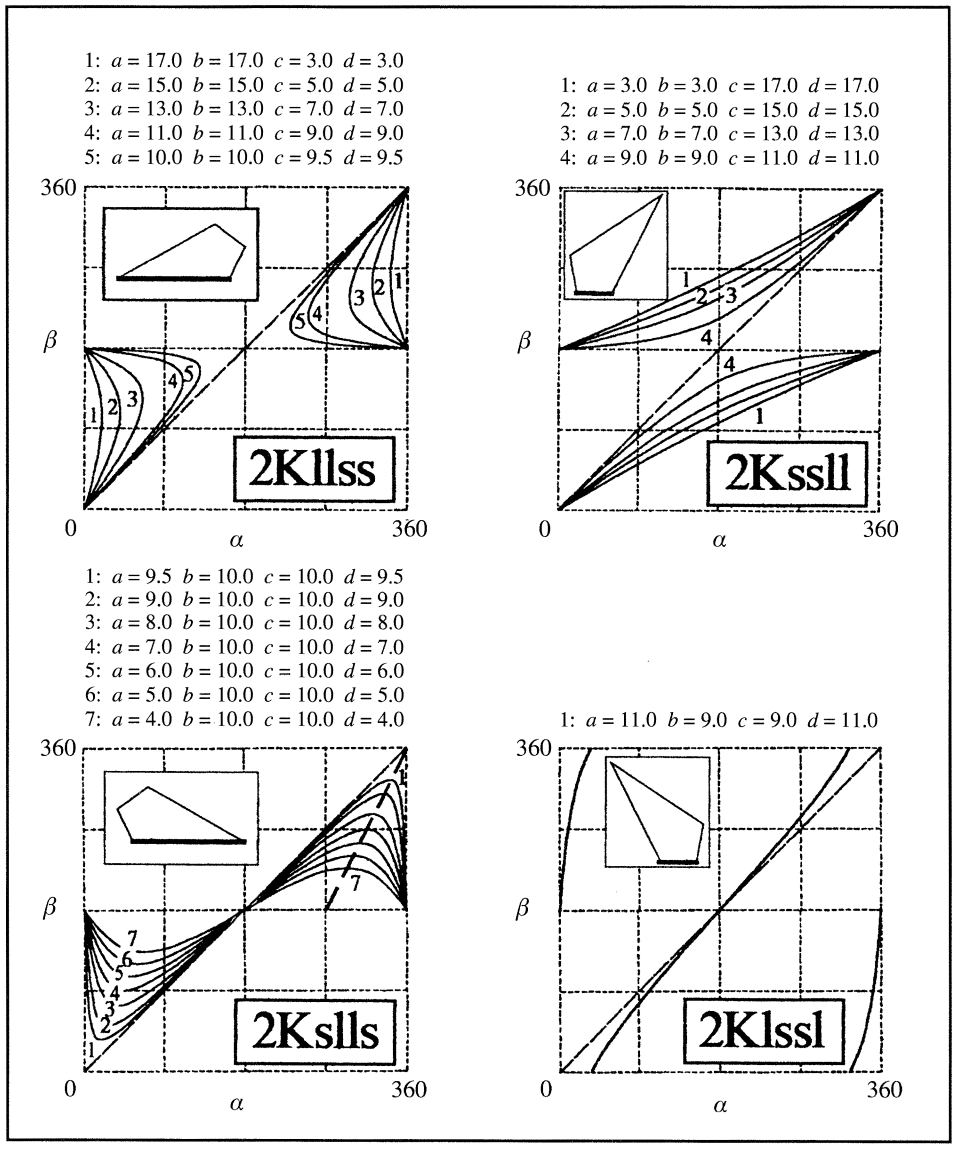

Figure 5. Transmission functions of isosceles (kite) linkages. In diagram 2Kslls values of bar lengths are given from Muller (1989). In this diagram, it is shown that the extreme values of the transmission functions lie on a straight line. The solid bar in the inset denotes the frame-link *b*, the left bar is the input-link *a*. The lines give the transmission functions for the outwards folding (kite) and inwards folding (deltoid) configurations. No crossed configurations exist. The codes are defined in table 2. Further explanation in text (§4*b*).

(*a*) *Parallellogram- or 2P-linkages*: (a = c) *and* (b = d)

In the non-crossed configuration, parallellogram linkages give a linear transmission of α to β over the [0,360°]-range. In the crossed configuration however, transmission becomes non-linear, especially for rhombus-like linkages. For example, in curve 4 (in figure 4) a small variation of α leads to a very large variation of β in the ranges $\alpha \in [0,20°]$ and $\alpha \in [340,360°]$ and a small variation of β leads to a large variation of α in the range $\alpha \in [90,270°]$. This enables also the possibility of a considerable change of transmission properties by only 'shifting the range' of input angles. A 'positive transmission' (i.e. α and β both increase or decrease) is obtained for a parallellogram linkage of the type 2Plsls, a 'negative transmission' (i.e. α increases and β decreases or vice versa) for a parallellogram linkage of the type 2Pslsl. In the parallellogram linkage, absolute 'transmission-stability' is obtained in the non-crossed configuration, implying that a change of the transmission by a change of the linkage parameters in 'evolution' cannot occur (or can be avoided), whereas in the crossed configuration evolution may lead to a very different transmission. In the latter configuration, the transmission may be very sensitive to a change of parameters.

Parallellogram linkages have no undetermined positions as the rhombus has. At the corresponding angles however 'branched positions' occur in which the linkage may change from its crossed to its non-crossed configuration.

Biological linkages with a positive transmission are discussed in §6*a*. An example of a conversely crossed linkage are the cruciate ligaments in the knee joint, discussed in more detail in §6*d*. It is noticeable that

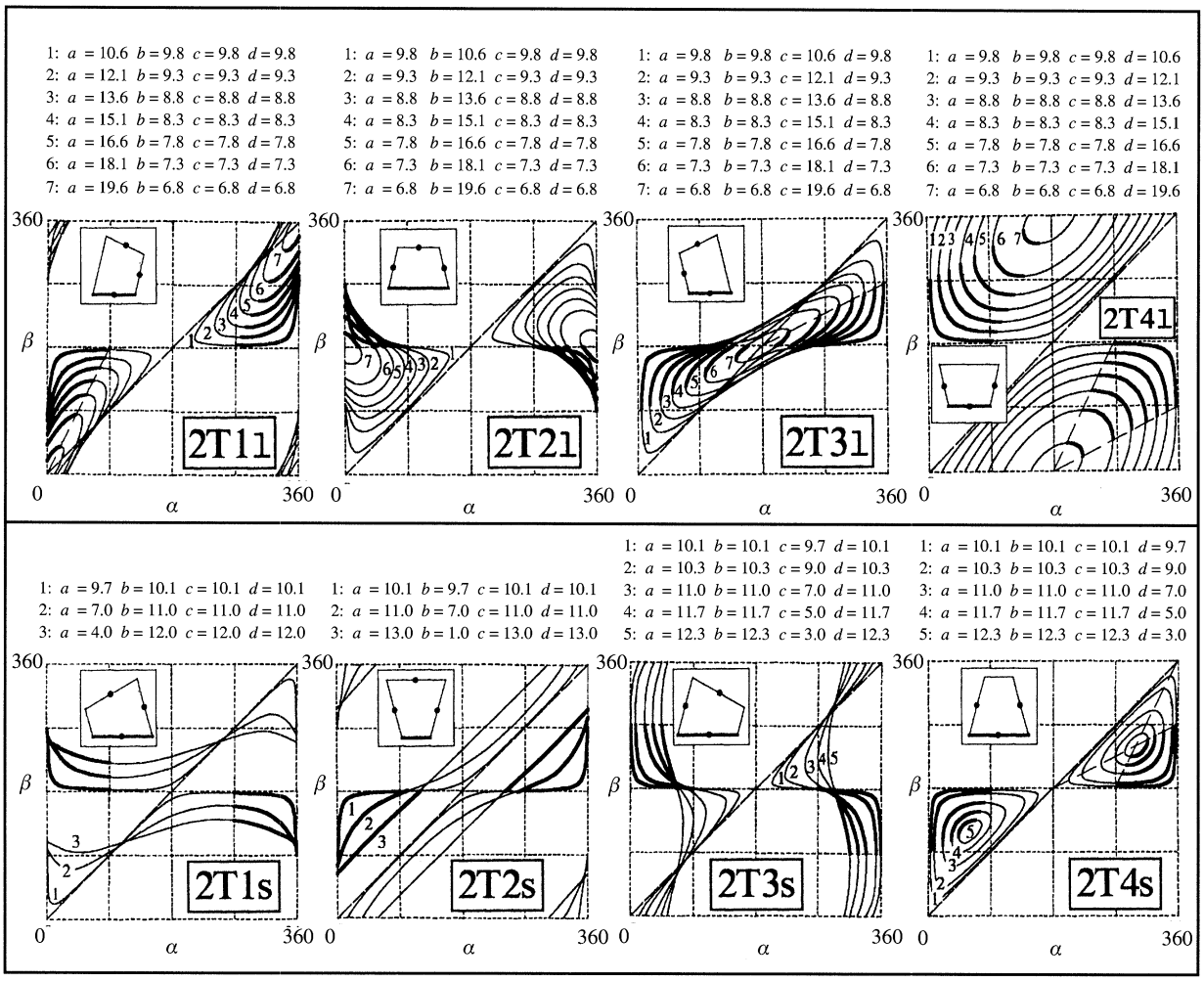

Figure 6. Transmission functions of trapezoidal linkages. The perimeter of the different linkages is kept constant. The thin lines give the transmission functions for the uncrossed configurations, the bold lines for the crossed configurations. Hatched lines indicate the values $\alpha = \beta$ and in some diagrams transitions from crossed to uncrossed configurations. The solid bar in the inset denotes the frame-link *b*, the left bar is the input-link *a*. Dots indicate equal bars. The codes are defined in table 2. Further explanation in text (§4*c*).

knee-prosthesis four-bar linkages are mostly uncrossed (see e.g. Hobson & Torfason 1974, 1975; Greene 1983), so in surgery-engineering, no advantage has been taken of the non-linear properties present in the natural system.

(*b*) *Isosceles-, Kite-, Deltoid- or 2K-linkages*: (**a = b** *and* **c = d**) *or* (**b = c** *and* **a = d**)

Regarded formally, the isosceles-linkage can be brought in a 'deltoid' (inwards folding) and a 'kite' (outwards folding) configuration. Usually, the names of the configurations are also used for the linkage. Four 'inversions' of isosceles-linkages can be distinguished. The inversions with a long base have similar, but rotated and shifted transmission curves (figure 5: 2Kllss and 2Kslls), the inversions with a short base can in a similar way be taken together (figure 5: 2Kssll and 2Klssl). Undetermined cases occur for $\alpha = 0 + k.360°$ (figure 5: upper diagrams) and $\beta = 180 + k.360°$ (figure 5: lower diagrams). No crossed configuration exists but the short bars may come to lie in line, forming a 'branched position' between deltoid- and kite configurations (figure 16). Folding linkages also exist for 3- or 4-parameter linkages (see §5*b*).

A well-known feature of the inversions 2Kssll and 2Klssl is that the range of movement of opposite bars over one cycle differs a factor 2 (Reuleaux 1983). The isosceles-linkage is the only constructionally 'bilaterally symmetric' four-bar linkage, which implies its biological importance. Applications in fish-head functional morphology are given by Muller (1989) who attempted to optimize the dimensions of the four-bar linkage with respect to functional demands for feeding (see §6*b*) and Aerts (1991) who extended the planar isosceles-model to a three-dimensional one to describe accurately its (quasi-) time-dependent behaviour.

(*c*) *Trapezoidal or 2T-linkages*: (**a = b = c**) *or* (**b = c = d**) *or* (**c = d = a**) *or* (**d = a = c**)

An overview of the eight possibilities in this class of linkages is given in figure 6. A first subdivision can be made in trapezoidal linkages with one relatively long

bar (figure 6: upper row) and trapezoidal linkages with one relatively short bar (figure 6: lower row). Further splitting, in different pairs of linkage types, can be easily read from the diagrams in figure 6. A particular feature of the linkages 2T*s (* = 1...4) is that two closed image-curves ('branches') exist, implying that the transmission cannot move along these two curves without dismounting the linkage (see §2).

The trapezoidal linkages also enable a 'locked position' from which the linkage can be triggered (figure 2, Muller 1987). Parallellogram- and isosceles-linkages do not possess this option but locking linkages are also possible with 3 and 4 parameters (see §§5*b* and 6*c*).

The linkages 2T4s and 2T11 are of importance in 'transient' movements e.g. in feeding pipefishes (Muller 1987). See §6*c* for more details.

In the literature, particular mechanisms have been considered as 'catastrophe-mechanisms' i.e. bistable mechanisms which may 'jump' from one state to another. An example is the click mechanism for wing-movements in insects as considered by Thomson & Thompson (1977). The wing-movements predicted by these authors are quite realistic and from a mathematical point of view the approach is very attractive. Nonetheless, it is in my view incorrect and misleading to speak of a 'catastrophe-mechanism' because all mechanical positions of the mechanism are feasible and actually existing during the movement. In real catastrophe-mechanisms, the 'catastrophe' consists of a non-feasible situation (Alexander 1982). Using linkages, the mechanical construction of a biological structure can be modelled much more realistically than a catastrophe-mechanism and asymmetrical movement curves can also be produced easily.

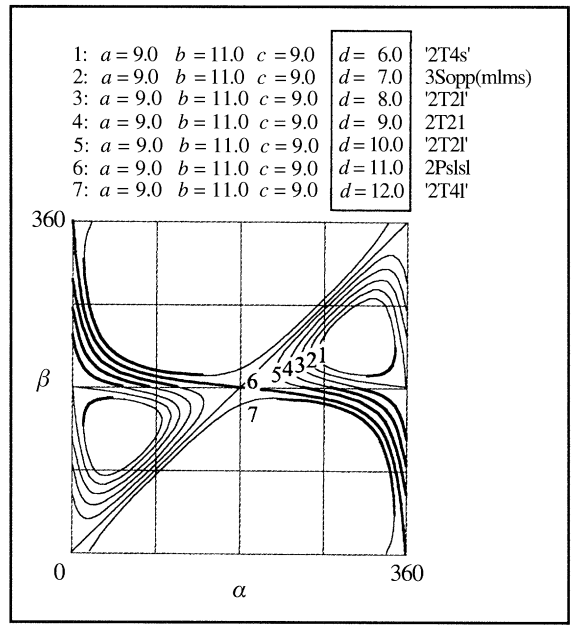

Figure 7. Example of a series of 3-parameter linkages. The short notation (code) of this particular series is 3Pslsl(4) which means: a 3-parameter linkage, based on the two-parameter parallellogram linkage 2Pslsl (see figure 4) in which bar 4 (= bar *d*) is varied. A complete overview of codes can be found in table 2. Codes within quotation-marks indicate the 2-parameter linkage type with a transmission function that resembles the transmission function of the linkage in question (approximate function cognate). The choice of the linkages corresponds to the series in table 5 (not the same bar-values chosen). The thin lines give the transmission function for the uncrossed configurations, the bold lines for the crossed configurations. Further explanation in text (§5*a*).

5. THREE-PARAMETER LINKAGES

(*a*) *Three-parameter series*

It is apparent that with three bar lengths the overview of movement possibilities is in danger to get lost. Figure 7 gives an overview of transmission curves of an arbitrarily chosen series of three-parameter linkages (i.e. 3Pslsl(4); for explanation see figure legend; for other codes, see table 2; for a general overview, see table 5). This series runs through some 2-parameter linkages and a linkage (figure 7: no. 2) that possesses unique properties compared to two-parameter linkages (see §5*b*). It would be valuable to dispose of an overview which gives all transitions in 3-parameter series. Then, the mechanical properties of a particular 3-parameter linkage could be judged e.g. from the closest transitional stages. This is discussed in detail in §§5*c* and *d*).

Another advantage of a series such as figure 7 is that it gives insight into possibilities, and non-possibilities (!), of evolutionary changes in the mechanical behaviour of biological linkages. Here this is only considered for changes in a single parameter (see §§5*d* and 6*e*).

Although the details of three- and four-parameter transmission curves are unique, the essentials of the system-behaviour can often be understood by comparing them with transmission curves of approximately similar 2-parameter- and 3S-linkages (figures 4, 5, 6, 9 and 10; see also §§5*b* and 6*c*). First, the real transmission function is determined using all four parameters. This transmission-curve is then compared with those of the simpler 2-parameter- and 3S-linkages. These linkages are indicated in figure 7 with quotation-marks (also in other figures; see table 2). Here, we obtain a powerful tool to rigourously simplify the mechanical analysis of biological systems, even to a single-parameter level. Dr E. A. Dijksman (personal communication) has proposed the term 'approximate function cognates' for such linkages (see also Dijksman 1975). It is widely appreciated that an admissible reduction in the number of parameters strengthens the explanatory power of a model. Examples are given in §6. The appearance or disappearance of parts of the transmission functions for slight deviations of the bar lengths of the real 4-parameter linkage to obtain the cognate two-parameter linkage does mostly not affect the essentials of the transmission (see e.g. figure 14: *Latimeria* and *Equus* and figure 17). In this paper, approximate function cognates are indicated by placing the code between quotation-marks (see figure 7).

(*b*) *Special linkages*

Linkage no. 2 in figure 7 cannot be compared with any 2-parameter linkage. An example of such a linkage in different positions is shown in figure 8 (left box). It has no crossed configuration and behaves in this respect as an isosceles linkage. It can be brought to a folded position because $(b–a) = (c–d)$ (or more generally: $(l–m) = (m–s)$, see table 3). Contrary to the isosceles linkages, undetermined positions do not exist. It behaves partly trapezoid-like (inbetween 2T4s and 2T2l; see figures 6, 7) but cannot be locked to form an immobile triangle. It has stretched in-line positions as in isosceles linkages and trapezoidal linkages but lacks overlapping ones as in trapezoidal linkages. This special 3-parameter linkage with opposite equal bars, with a length between the longest and the shortest bar, is referred to as a 3Sopp-linkage (table 2). As described above, its properties can be considered being inbetween an isosceles linkage and a trapezoidal linkage. All 3Sopp-linkages are listed in table 3. Their transmission curves can be found in figure 9.

The only other possibility of a 3S-linkage has two adjacent bars of equal length. Some positions of a 3Sadj-linkage are shown in figure 8. The eight possibilities for 3Sadj-linkages are listed in table 3. Transmission curves are shown in figure 10. The properties of 3Sadj-linkages are inbetween a parallellogram and a trapezoidal linkage. A crossed configuration and branched positions exist as in parallellograms. Locked-, stretched in-line- and overlapping in-line positions are as in trapezoidal linkages.

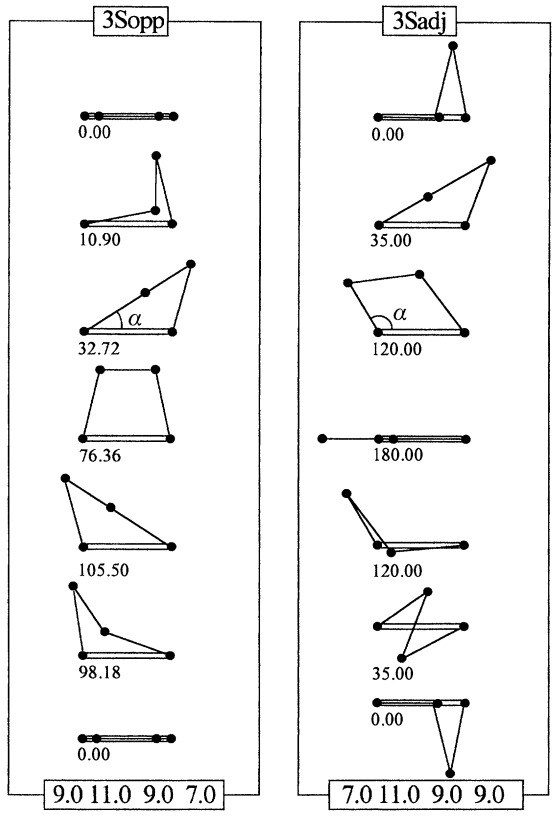

Figure 8. Some positions of the two types of special 3-parameter linkages (3S-linkages). The linkages correspond to linkages in tables 3 and 5 and figures 9 and 10. The input angle α is drawn in the third diagrams and numerically indicated near each diagram. Further explanation in text (§5*b*).

Table 3. *Overview of all possible 3S-linkages*

l = longest bar, s = shortest bar, m = intermediate bar.

type code	linkage	example
3Sopp		
3Sopp(msml)	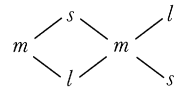	9.0 7.0 9.0 11.0
3Sopp(mlms)		9.0 11.0 9.0 7.0
3Sopp(smlm)	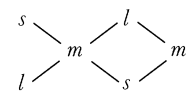	7.0 9.0 11.0 9.0
3Sopp(lmsm)		11.0 9.0 7.0 9.0
3Sadj		
3Sadj(mmsl)	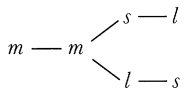	9.0 9.0 7.0 11.0
3Sadj(mmls)		9.0 9.0 11.0 7.0
3Sadj(smml)	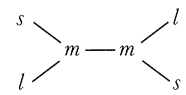	7.0 9.0 9.0 11.0
3Sadj(lmms)		11.0 9.0 9.0 7.0
3Sadj(slmm)	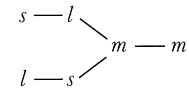	7.0 11.0 9.0 9.0
3Sadj(lsmm)		11.0 7.0 9.0 9.0
3Sadj(mslm)	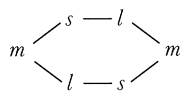	9.0 7.0 11.0 9.0
3Sadj(mlsm)		9.0 11.0 7.0 9.0

From the above description, it follows that only linkages which satisfy the condition: $(l+s = 2m)$ are 3S-linkages.

The special linkages with four different bar lengths (4S) can easily be derived from the **3S**-linkages. This is shown in figure 11. The four parameter linkages are obtained by elongating or shortening adjacent bars in the folded and branched positions. A folding 3-parameter special linkage can only be modified in a folding 4-parameter linkage or in a 2-parameter folding one (isosceles linkage). The shortest (s) and longest (l) bars remain always opposite. The crossing linkage also preserves its character and the shortest and longest bars remain always adjacent.

All special linkages discussed in this section correspond to type 3 linkages in the engineering classification (table 1; see also pp. 230, 231 in Dijksman 1976). The method for deriving them by a parameter consideration, as detailed above, is more refined and exposes aspects of their mechanical properties which are not immediately apparent from the engineering consideration. Examples of 3Sopp- and 3Sadj-linkages in biology are given in §§6*a* and *b*.

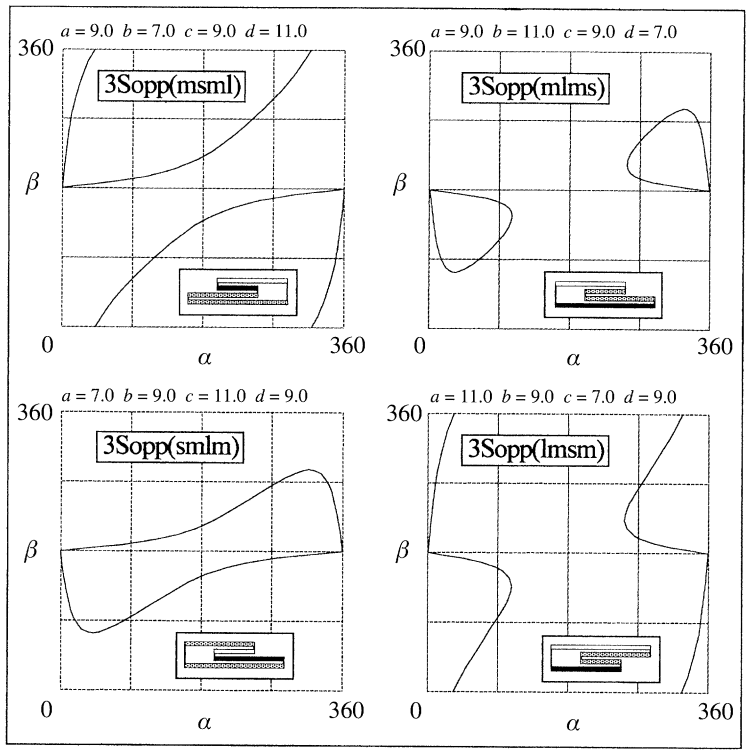

Figure 9. Transmission functions of the special 3-parameter linkages 3Sopp (two opposite bars are equal; folding linkages). The insets give a scheme of the linkage in a folded position. Black bar: frame-link, white bar: input-link. An overview of these linkages is given in table 3. The choice of the linkages corresponds to table 5. Further explanation in text (§5*b*).

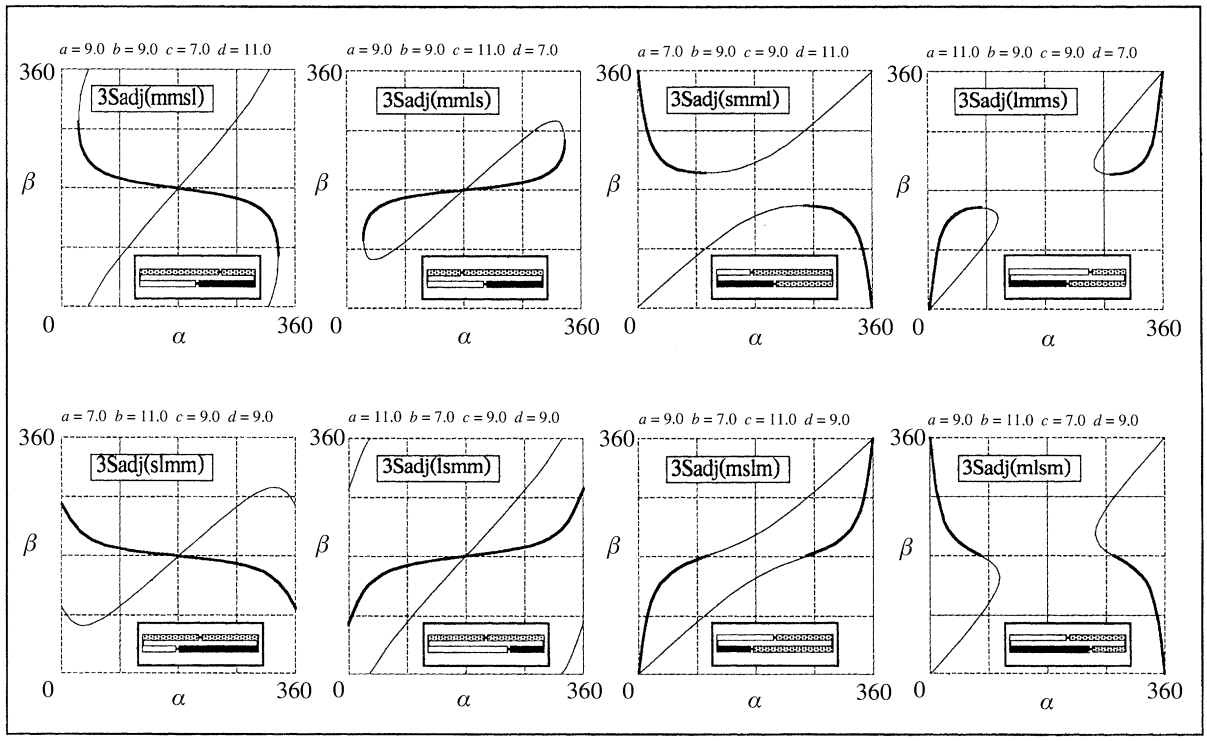

Figure 10. Transmission functions of the special 3-parameter linkages 3Sadj (two adjacent bars are equal; crossing linkages). The insets give a scheme of the linkage in a branched position. Black bar: frame-link, white bar: input-link. An overview of these linkages is given in table 3. The choice of the linkages corresponds to table 5. Further explanation in text (§5*b*).

(*c*) *Three-parameter transitions*

In this section, the question is addressed of what consequences an evolutionary change of a particular bar of a four-bar linkage may have on the mechanical functioning of a system. It was shown that in a three-parameter series (§5*a*) transitions to 2-parameter- and 3S-linkages occur. Transitions in Grashof conditions are also met and so transitions in crank- and rocker-movement. Table 5 lists these transitions for all 3-parameter series which originate from the fourteen two-parameter cases. This table was obtained by a computer programme which generated linkages of interest. The programme works as follows. Two different 3-parameter linkages of a particular series are required as input. This enables the programme to determine which bar is variable (i.e. which column in the series, see figure 7). Then, following the conditions of table 4, five different linkages were generated. Additionally, at each Grashof transition, two linkages were generated to show the transition. This was done for all permutations of bars. A second programme deleted all identical linkages per category which were superfluously generated by the first programme. All linkages were classified following the Grashof- and the parameter-classification. So, for thousands of initially unsurveyable linkages, only the relevant transitions in mechanical behaviour were selected.

Table 5 (in Appendix 3) gives a complete and comprehensive overview of all these possible 3-parameter transitions. It gives insight into mutual relations between different four-bar linkages and therefore may be used as a 'field-guide' for biologists who study evolutionary transitions. With the help of the transmission functions (figure 4, 5, 6, 9 and 10), it enables evaluation of evolutionary possibilities and difficulties for changes in mechanical behaviour. I selected the following possibilities.

1. From 3P-series (i.e. 3-parameter series based on 2-parameter parallellograms), 2P-, 2T- and 3Sopp-linkages may be obtained.
2. From 3K-series (i.e. 3-parameter series based on 2-parameter isosceles linkages), 2K-, 2T- and 3Sadj-linkages may originate.
3. From 3T-series (i.e. 3-parameter series based on 2-parameter trapezoidal linkages), all types may follow.

Observing, for example, the 3Pslsl(1)-series in table 5 with the input bar a varying from short to long, it reveals that the linkages for relatively small values of bar a change from cr- linkages, via a single cc-linkage to rc-linkages. So, bar a changes from crank to rocker, and bar c does the reverse. This has implications for the allowed absolute values of α and β, and for the allowed ranges of $\Delta\alpha$ and $\Delta\beta$ in the biological system: when changing in evolution, the bars are meeting other movement-possibilities and -limitations which e.g. may jam the mechanical behaviour of the system. The cc-linkage (2Pslsl: $a = 9$) possesses branching positions which may cause instability in the transmission. The avoidance of such a linkage requires a special pathway in evolution, e.g. via 4-parameter-linkages, via a limitation of the α-range in the cc-linkage (see §5*d*), or even by coupling of the cc-linkage to another linkage. At relatively large values of bar a, the linkages change to rr-linkages via a 3Sopp-linkage. This enables the evolution of a linkage with folding properties.

For folding linkages in which the folding charac-

Table 4. *Cases for the generation of new four-bar linkages in a 3-parameter series*

(Suppose that the b-bar is the variable bar (V) in the series. The other bars are constant. New linkages can be generated: (i) by making adjacent bars equal; (ii) by making 3S-linkages following the concerning rules (§5(*c*). A choice of the variable bar can be made by cyclical change of the input bars. The result is the generation of five different linkages (V1...V5). This is elucidated in the scheme below.)

adjacent bars of bar b equal
V1 = a
V2 = c
(3Sopp)-configurations
$d-a=c-b \longrightarrow b=c-d+a$
$d-a=c-d \longrightarrow b=c-d+a$
so:
V3 = $c-d+a$
(3Sadj)-configurations
$a+b=c+d \longrightarrow b=c+d-a$
$b+c=d+a \longrightarrow b=d+a-c$
$c+d=a+b \longrightarrow b=c+d-a$
$d+a=b+c \longrightarrow b=d+a-c$
so:
V4 = $c+d-a$
V5 = $d+a-c$

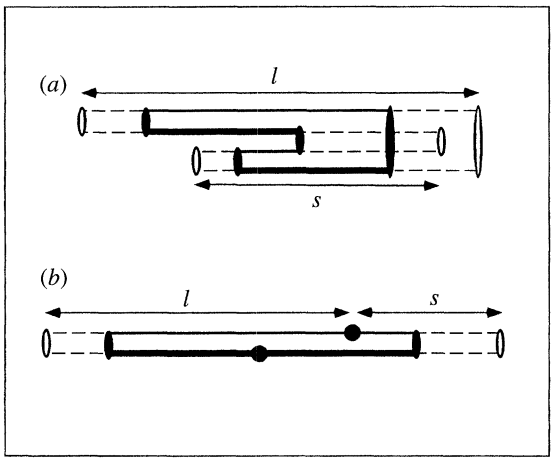

Figure 11. The derivation of special 4-parameter linkages from special 3-parameter linkages. (*a*) (3Sopp)-systems to 4S-systems; (*b*) (3Sadj)-systems to 4S-systems. The equal (intermediate) bars (*m*) are drawn bold. l = longest bar, s = shortest bar. Change of bar-lenghts may be in all directions and combinations in folded (3Sopp) resp. branched (3Sadj) positions. The 4S-linkages may be divided in 'opp' and 'adj' linkages when the longest and shortest bars are opposite or adjacent. All these linkages correspond to 'Type 3 linkages' in table 1. Further explanation in text (§5*b*).

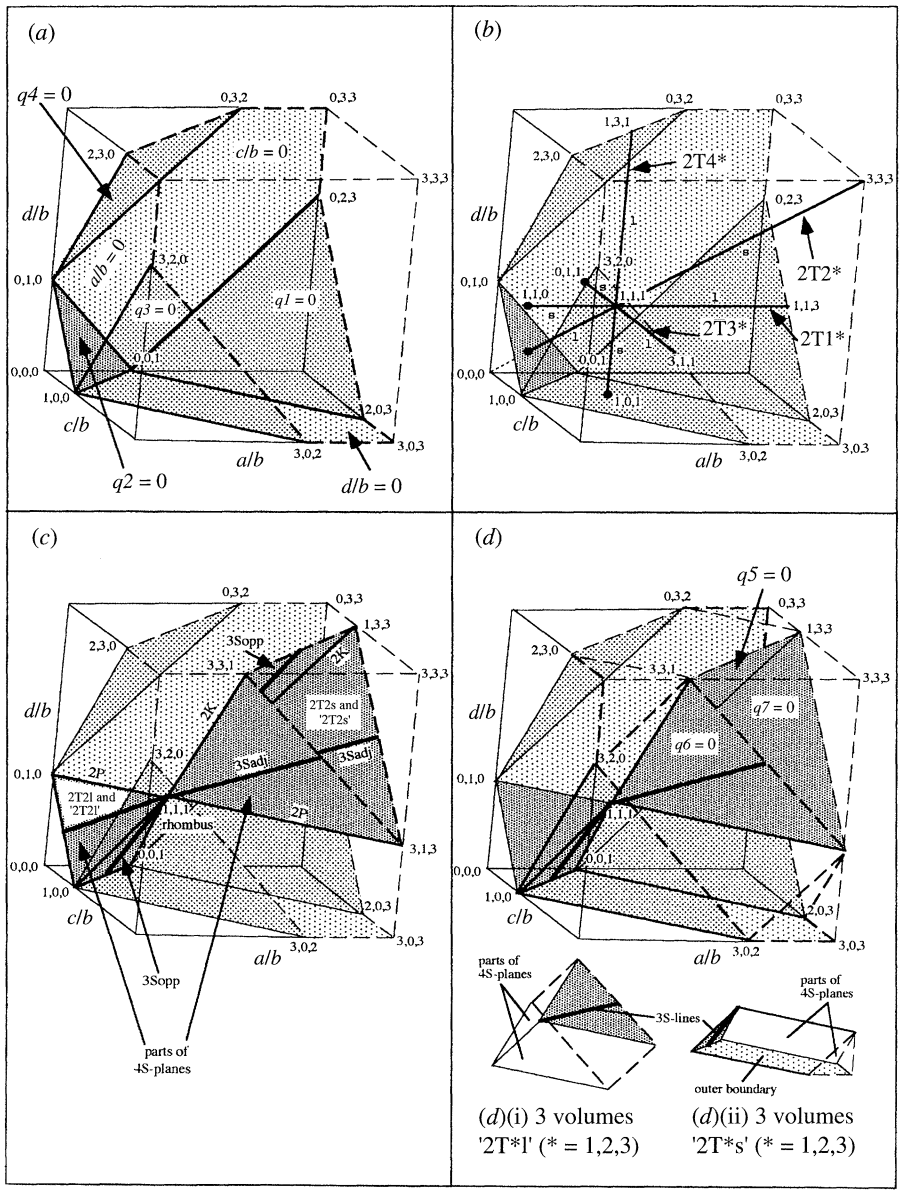

Figure 12. The three-dimensional parameter solution space developed by Hain (1964) and Barker (1985) with linkage-characterizations of the present classification. The (dimensionless) co-ordinates in the diagrams may help to follow the orientation of lines and planes in three dimensions. Dashed lines: spaces limited by the cube. (*a*) Outer boundary of all 4-bar systems, limiting the space wherein all four-bar linkages can be realised. (*b*) 2T**-linkages can be realised along the orthogonal and diagonal lines in the solution space. 'l'- and 's'-linkages are indicated near the line parts. These parts are separated by the rhomboid linkage in point (1,1,1). (*c*) and (*d*) further explorations of the solution space: (*c*) rhombus, 2P-, 2K-, 3S-, 4S- and '2T2*' systems; (*d*) 3S-, 4S- and '2T**'-systems. The line 2P runs along the scaled values $a = c$, $d = 1$. The 2K-lines are obtained for $a = d$, $c = 1$ and $c = d$, $a = 1$. The 3S-lines are the bisectors of the planes forming the tetrahedrons. In diagrams (*d*)(i) and (*d*)(ii), the (*) in the codes may be (1,3,4) as (* = 2) is contained in the tetrahedrons (see diagram (*c*)). Comparison of diagrams (*d*)(i) and (*d*)(ii) with diagram (*b*) reveals in which volumes the 'l'- and 's'-linkages are found. Further explanation in text (§5*d*).

teristics should be preserved, there are limited possibilities for evolutionary transitions. Table 5 shows that the folding properties are easily lost (see §6*e*). A pathway along 4-parameter linkages is possible (see figure 11 and §5*d*).

In the 3T-series, transitions sometimes are via a rhombus (see e.g. 3T11(1) in table 5). When, for instance, crossed positions of a linkage would be essential, an evolutionary approach or transition in this range would be very difficult or even a real barrier would be met. This rules also for 3P-series in which 3Sopp-linkages occur.

As mostly the essentials of the mechanical functioning of four-bar linkages already can be approximated by 2-parameter and 3S-transmission functions (see §5*a*), the 3-parameter transitions in table 5 give sufficient flexibility to study possible evolutionary trends in many biological systems (e.g. those discussed in §6). Some caution is however required. This is discussed in the next section in which an

extension of the above analysis to 4-parameter considerations is made.

(*d*) *Three- and four-parameter transitions*

This section can be omitted at first reading as it requires a detailed consideration of the three-dimensional parameter space of four-bar linkages developed by Hain (1964) and further explored by Barker (1985). The aim of this section is to provide a more general scheme that gives a deeper insight in the results of table 5.

Hain's parameter space is constructed as follows. First, the lengths of the bars of a four-bar linkage are scaled with respect to the frame-bar, i.e. all bars are divided by the length of bar b. In the rest of this section, only scaled bar-lengths will be considered. Now, the scaled values of bars a, c, and d can be plotted in a three-dimensional coordinate system (figure 12). In this system, possibilities and limitations for the construction of particular four-bar linkages can be investigated.

The outer boundary (figure 12*a*) which limits the possible construction of any four-bar linkage is formed by the trivial conditions: $a = 0$, $c = 0$, $d = 0$, and by the equations:

$$q1 = (+a) - b - c - d \geqslant 0$$

$$q2 = -a(+b) - c - d \geqslant 0$$

$$q3 = -a - b(+c) - d \geqslant 0$$

$$q4 = -a - b - c(+d) \geqslant 0$$

(these and the following equations can be checked easily by taking special cases, e.g. intersections with the coordinate cube). The rhomboid linkage (all bars equal; see figure 3) is located in the point (1,1,1) (figure 12*c*).

Within the outer boundary, all possible 2T**-linkages are represented by straight lines (figure 12*b*). Note that 3T**-series along these lines (so, 3Tx*(x), $(x = 1 \ldots 4)$) have to contain only two parameters (see figure 13*b*) and so are no 'true' 3-parameter series. They only pass the rhombus-transition (figures 12*b*, 13*b*). For completeness, they are included in table 5.

The conditions for the construction of 4S-linkages (or type 3-linkages; see table 1) are:

$q5 = (a+c) - (b+d) = 0$ (4Sopp i.e short and long bars opposite; figure 11*a*)

$q6 = (a+d) - (b+c) = 0$ (4Sadj i.e short and long bars adjacent; figure 11*b*)

$q7 = (c+d) - (b+a) = 0$ (4Sadj idem; figure 11*b*).

These three equations determine a surface within the outer boundary consisting of two tetrahedrons and the extensions of the planes forming these tetrahedrons (figure 12*c*, *d*). Particular straight lines on this surface represent the 2P-, 2K- and 3S-linkages (figure 12*c*). Crank-rocker-transitions may only occur at this surface (Barker 1985).

All other linkages in the parameter space are more or less trapezoid-like, obviously depending on their position with respect to the lines and planes mentioned above. Two examples are still worth to be mentioned here: within the 'small tetrahedron', the scaled bars a, c and d are always smaller than the frame b, so we obtain 2T2l- and '2T2l'-linkages. Analogously, within the 'large (infinite) tetrahedron' 2T2s- and '2T2s'-linkages are present (figure 12*b*). Other particular volumes and lines are shown in figures 12 and 13 and are not treated in detail here.

An overview of a variation series of table 5 is obtained by considering the intersection of the parameter space by a diagonal plane (because in table 5 always at least two bars are equal). An example is shown in figure 13 (i.e. for $a = c$). From figures 12 and 13, it is now possible to judge more closely some merits and limitations of table 5.

When one would take a variation series in a plane parallel to the plane in figure 13, most of the 2-parameter and 3S-linkages of figure 13*b* would not be found. Instead of the rhombus, one would find single 2T1*- and 2T3*-linkages. Two 2K- and two 3Sadj-linkages would be obtained. 4S-linkages would be found at the intersections with the 4S-planes of the tetrahedrons. At sufficient distance of the plane of figure 13, the whole 'small tetrahedron' would be missed however. So, despite still varying a single bar length and taking the relation between two other bar lengths to be constant, the chance of obtaining a 2- or 3-parameter linkage would be different and often smaller than in figure 13*b*.

Another example is to take variation series e.g. in a plane parallel to the plane $[a,c]$ for $d = 1$ (figure 12*b*, *c*). Now, 2P- and 2T-linkages can be found exclusively, i.e. no 3S- and 4S-linkages. The latter linkages, together with 2K-linkages, are found for other values of d, i.e. other parallel-planes, but also here the chances of obtaining such linkages is relatively small compared to figure 13*b*.

Finally, one may choose variation series in the 4S-planes (figure 12*c*), so preserving folding or branching properties. This includes in itself already a rather serious limitation. Also in this case, the same conclusion for the above two examples holds.

The general conclusion of the above discussion is that the variation series of table 5 provide a satisfactory first and rather simple clue to study evolutionary variations of bar-lengths which may lead to transitions between different four-bar linkages or transmission properties of linkages. The use of the parameter space of figure 12 is absolutely essential where a four-parameter approach cannot be avoided! Table 5 and figure 13 may then help to understand in which part of the parameter space a transition may take place and what kind of linkages one may expect to find there. A more general engineering approach for variation of four bar lengths can be found in Hain (1964). Occasionally, a simultaneous variation of two bar lengths is possible as e.g. in the case of snout elongation (see §6*a*). I have however strong reservations against more 'exotic' examples of simultaneous variation of bar lengths (see §6*e*).

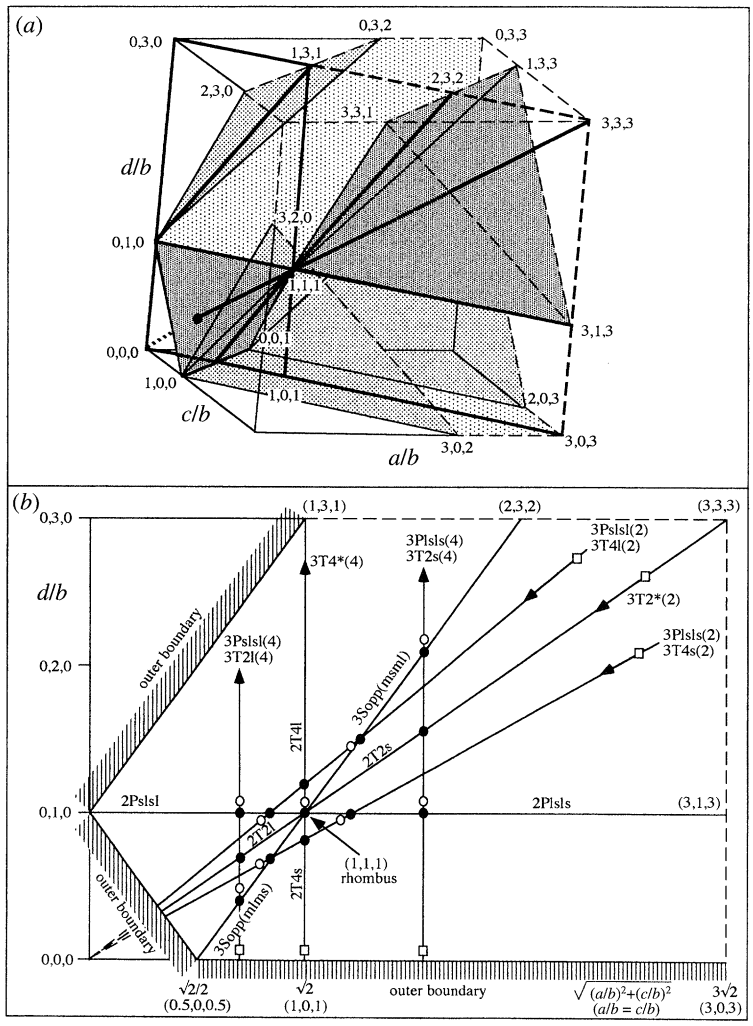

Figure 13. An intersection of the solution space of figure 12 by a diagonal-plane, elucidating the composition of three-parameter series of table 5. (*a*) the plane in the solution space. Lines in the plane are drawn bold. (*b*) the typification of linkages and three-parameter series in the plane. The rhombus-linkage separates the linkage types which are indicated at the lines. All possible three-parameter series of table 5 in this plane are indicated by arrows. Black dots indicate the 2-parameter- and 3S-linkages met in these series. Open squares indicate the start-linkages of the 3-parameter series in table 5. Open circles indicate the crank-rocker transitions shown in table 5. All lines originating from the origin (0,0,0) have a constant (*a*,*c*,*d*)-ratio, so the *b*-bar varies. Co-ordinates in the three-dimensional space (so corresponding to diagram *a*) are indicated within parentheses. Further explanation in text (§5*d*).

6. BIOLOGICAL SYSTEMS

The mechanical features of the biological systems described in this section were partly published by different authors and are partly original. All the examples mentioned have been carefully checked in original material by M.M.

(*a*) *Approximate linear transmission*

This section deals with positive transmission systems (see §2). Although positive transmission may be strongly non-linear (§4*a*), here only systems with an approximately linear (proportional) transmission in the working range will be considered.

Examples are shown in figure 14, including: (i) the opercular mandible depression mechanism in fishes (Anker 1974; Barel *et al.* 1977; Aerts & Verraes 1984) in which elongation of the snout of a fish, and so change in type of the four-bar linkage, does have little influence on the transmission function (Barel *et al.* 1975); (ii) the jaw movement mechanism in labrid fishes (Westneat 1991, 1994); (iii) the skull-levation mechanism in the coelacanth *Latimeria* (Alexander 1973), reptiles (Frazzetta 1962, 1966) and birds (Bock 1964); and (iv) the plantaris system ('reciprocal apparatus') in the hind legs of ungulates (Badoux 1975; Moolenaar 1983).

Although superficially these systems seem to be not very different in transmission properties, figure 14*b* shows that they in fact belong to different classes. Their transmission curves differ also in slope and working range. From the transmission curve 6 (in figure 14*b*), it is apparent that *Latimeria* possesses the only known biological linkage which is close to a 3Sadj-linkage (compare to figure 10: 3Sadj(mmls)) and is also in this respect a remarkable animal. The theory developed in the previous sections considerably helps in the investigation of these aspects.

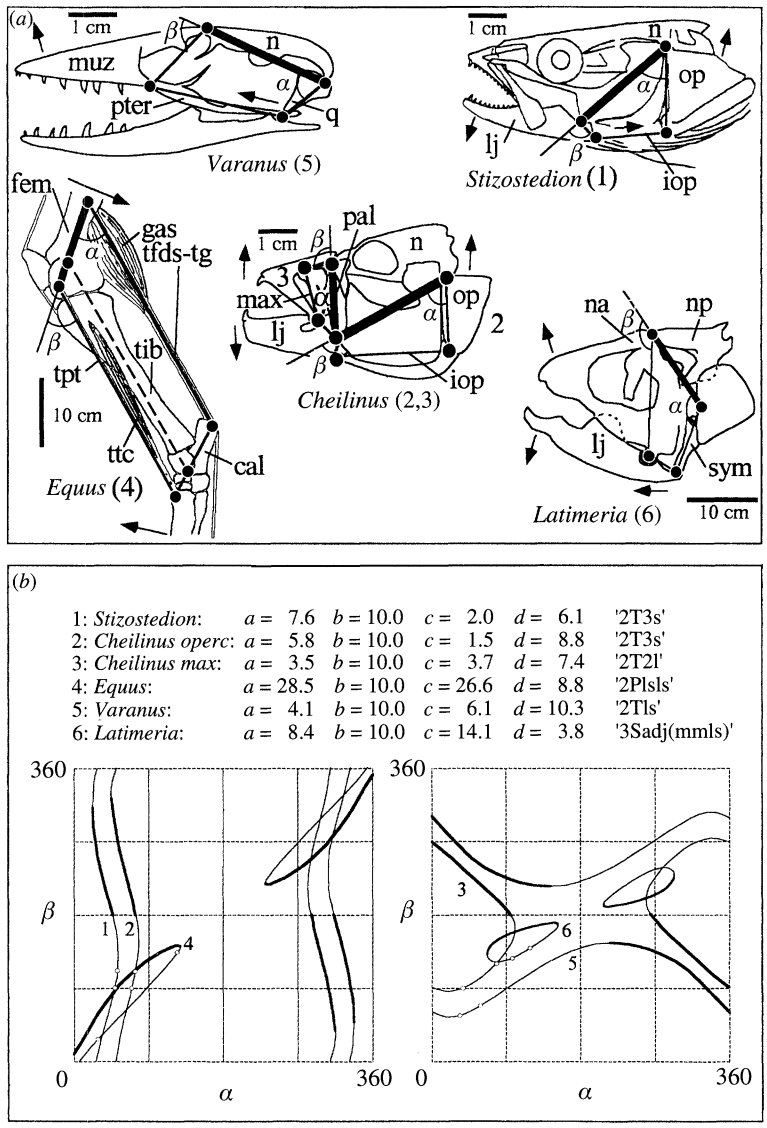

Figure 14. Examples of biological four-bar systems with approximately linear positive transmission functions in the working range. (*a*) Structures; (*b*) Transmission curves. Frame bars *b* are drawn bold. Bold curves give the transmission function for the crossed configuration. The approximate 2-parameter function cognate linkages are indicated in diagram (*b*) within quotation marks. The approximate working ranges are indicated by small open circles. Normalized linkage dimensions are consistent with lengths in the present pictures and may be somewhat different from the data of the original authors. This does not affect the results. $\alpha_i = \alpha$ in initial position, $\alpha_f = \alpha$ in final position. Further explanation in text (§6*a*).

animal and linkage no.	anatomical names of bars (abbreviations in Appendix 2)	approximate working range (°) α_i	α_f	reference (partly cited)
Stizostedion (*1*) (pike-perch)	*a* = op, *b* = n-sus, *c* = lj, *d* = iop-lim	30	40	Osse (1983)
Cheilinus (*2*) (wrasse)	*a* = op, *b* = n-sus, *c* = lj, *d* = iop-lim	50	60	Westneat (1990)
Cheilinus (*3*) (wrasse)	*a* = lj, *b* = n-sus, *c* = pal, *d* = max	40	80	Westneat (1990)
Equus (*4*) (horse)	*a* = tg-tfds, *b* = fem, *c* = tpt, *d* = cal, additional link: tib	30	145	Badoux (1975) Moolenaar (1983)
Varanus (*5*) (monitor, lizard)	*a* = q, *b* = pu, *c* = muz, *d* = pter	30	65	Frazzetta (1962)
Latimeria (*6*) (coelacanth)	*a* = ih-sym, *b* = np, *c* = na-pal-q, *d* = lj	125	100	Alexander (1973)

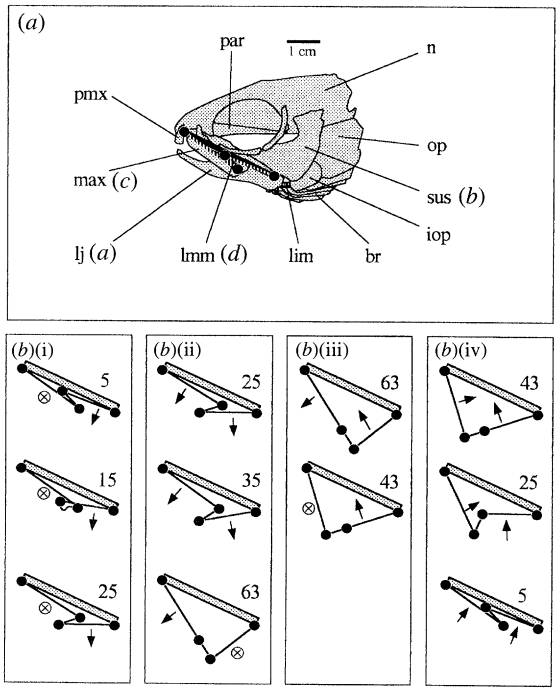

Figure 15. An example of a biological '3Sopp(mlms)'-linkage. (*a*) the linkage in a lateral view of the rainbow trout, *Oncorhynchus mykiss* (= *Salmo gairdneri*) (modified after Aerts & Verraes, 1987). The linkage consists of: (1) the lower jaw (bar *a*), (2) the suspensorium (bar *b*), (3) the maxillare (bar *c*) and (4) the maxillo-mandibular ligament (bar *d*). During movement, bar-sequences change, see text. The angle between the lower jaw- and suspensorium-bar is indicated near the diagrams. The ⊗-sign denotes a stationary state of a bar. Normalized linkage dimensions are (*a*) : (*b*) : (*c*) : (*d*) = (53) : (100) : (69) : (21). The transmission curve of this 4-parameter linkage closely resembles the transmission curve of the 3Sopp(mlms)-linkage: (*a*) : (*b*) : (*c*) : (*d*) = (60) : (100) : (60) : (20) (see figure 17). (*b*)(i–iv) some positions during different stages of movement. Note that in- and output bars change in different stages. Anatomical abbreviations in Appendix 2. Further explanation in text (§6*c*).

(*b*) *Folding mechanisms and force amplification*

A folding 4S- four-bar linkage that closely approximates the 3S-type: 3Sopp(mlms), is found in the mechanism that moves the maxillare in teleost fishes (figure 15). This mechanism was described for the first time by Alexander (1967) in the trout, *Salmo trutta*, and more rigorously by Aerts & Verraes (1987) in the rainbow trout *Oncorhynchus mykiss* (Wahlberg) (= *Salmo gairdneri* Richardson). The present analysis of the system is based on data of these authors and on some new discoveries of M.M.

The opening and closing movements of the mouth can be split up in four phases. In the first phase (figure 15*b*i) the lower jaw starts to depress. As the ligamentum maxillo-mandibulare (lmm) is not taut, the maxillare remains stationary. In this phase, the distal point of the *lj*-bar moves merely from a dorsal to a ventral position of the maxillare. An α of 25° marks the end of this phase i.e. when the lmm-bar has just become taut and a real four-bar linkage has been formed.

A second phase is drawn in figure 15*b*ii. The *lj*-bar is now the input-bar of the linkage. Further depression of this bar causes a forward rotation of ca. 22° of the maxillare. At an α of 63°, the lower jaw reaches its maximal depression.

In the third phase of the movement (figure 15*b*iii), the maxillare continues forward rotation by its inertia. In fact, the maxillare now becomes the input-bar of the linkage. It is interesting that the type of the linkage remains the same (which would not have been the case when the linkage would have been a isosceles linkage). At an α of 43°, the maxillare reaches it maximal forward rotation, 13° more than in phase 2. Obviously, the rotation-possibilities of the maxillare are dependent on the lengths of the bars. Back-rotation of the maxillare takes place in the fourth phase of the movement (figure 15*b*iv). The lower jaw is now again input-bar. At the end of this phase, the distal point of the *lj*-bar has reattained its position dorsally of the maxillare.

A peculiarity of the system is that, owing to the presence of a non-rigid bar (i.e. the lmm-bar), in each of the movement-phases in fact different mechanical systems are used (although their dimensions are approximately equal). This explains that the distal point of the *lj*-bar has to be dorsal of the *max*-bar in the rest situation to make the linkage in phase 4 functional and that it first has to be moved to a ventral position of the *max*-bar (phase 1) to make the linkages in phases 2 and 3 functional.

In physics, 'amplification' is mostly used when a quantity is enlarged by external supply of energy whereas enlargement without energy-supply is denoted by 'transformation'. This would be confusing in this article because 'transformation' is used for other purposes (see §2). So here the word 'amplification' will be used to denote an enlargement of a quantity (e.g. force), irrespective of the energy.

A four-bar linkage that enables force-amplification is found in the suspensorium abduction system in teleost fishes (figure 16) and has been described by Muller (1989). It is an isosceles linkage of the type 2Kslls. Transmission curves can be found in figure 5. Force-amplification occurs when the hyoid bars are close to the in-line position (figure 16*b*, *c*; see also §4*b*).

In four-bar linkages with approximate in-line bars, a rather weak input force may produce a comparatively very large output force (theoretically infinitely large). This is explained in figure 16*c*i–iv where forces (↠) and movements (→) are considered in different four-bar linkages. A force calculation in an isosceles linkage can be found in Muller (1989). It would be superfluous to repeat this here.

Figure 16*c*i considers the hyoid-jaw linkage described by Muller (1989). In the left picture, abduction of the linkage takes place, in the right one adduction. 'Muscle' forces F_x are transformed to linkage forces F_y. In the left picture of figure 16*c*ii, the hyoids are not in-line giving a relatively small adduction force (F_y). In the right picture, the hyoids are almost in-line giving a very large adduction force tending to infinity when the hyoids are in-line (limit case). The movements of point P are then rather small. A comparable force consideration can be found in Nash (1977: problem 1 : 14).

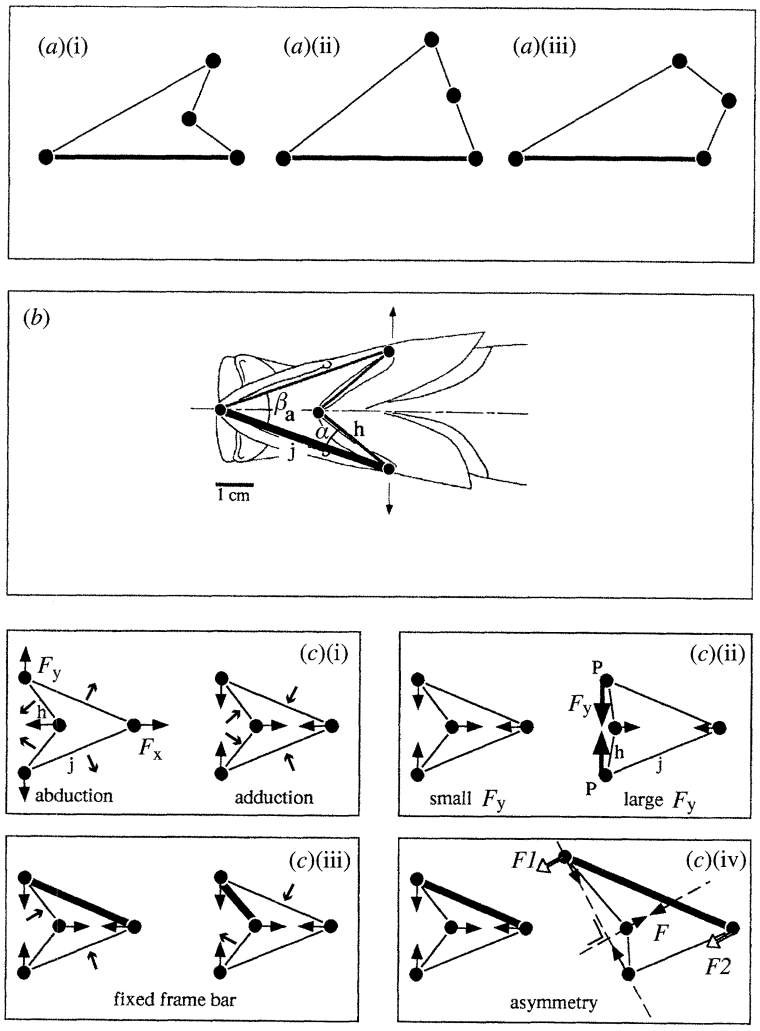

Figure 16. An example of a biological isosceles linkage. (*a*)(i) deltoid or inwards folding configuration; (*a*)(ii) in-line or aligned configuration; (*a*)(iii) kite or outwards folding configuration; (*b*) The linkage in a ventral view of the horse-mackerel, *Trachurus trachurus* (after Muller 1989). The linkage consists of the hyoids (*h*) and the lower jaw-suspensorium complex (*j*). In this example, the ratio h/j is ca. 0.57. The angle α is the input angle which is driven by the sternohyoid-, hypaxial-, and epaxial muscles, the angle β_a (supplement of β) represents the suspensorial abduction. Anatomical abbreviations in Appendix 2. (*c*)(i–iv) Diagrams, relating forces (➔ and outlined arrows) and movements (→) in different four-bar systems with approximate in-line bars. Frame bars *b* are drawn bold. F_x = force in x-direction, F_y = force in y-direction. Further explanation in text (§6*b*).

Figure 16*c*iii shows that, when a frame-bar is fixed (2 possibilities), the movements of the bars may change but the forces (F_x and F_y) remain the same. Figure 16*c*iv gives a transition from a symmetrical linkage to an asymmetrical one. As long as opposite forces are in-line and equal, the direction of their lines of action may be chosen arbitrarily. However, the forces corresponding to F_x and F_y of figure 16*c*i must remain orthogonal, also in diagram 16*c*iv. The force F (➔), acting on the frame-bar, may be replaced by the forces $F1$ and $F2$ (outlined arrows; not to scale).

Another (lower jaw)-(maxillare) system is the coral crushing apparatus of parrotfishes (e.g. *Pseudoscarus forsteni*: see figure 17, modified after Van Dobben 1935). The jaw mechanism of this fish is formed by a trapezoidal four-bar linkage. During biting (closing), this linkage consists of: the maxillare (bar *a*), the suspensorium (bar *b*), the articulare (bar *c*) and the dentale (bar *d*). In other scarids, the articular and dental bones are more or less grown together and the coupler bar is formed by the maxillo-mandibular ligament (compare *Oncorhynchus*, see above). Opening of the jaws is caused by a retraction-force of the interoperculum (F_{io}; outlined arrow; see §6*a*), closing is caused by a force exerted by the adductor mandibulae (F_{am}) (figure 17*a*ii). The adductor mandibulae muscle fibres act directly on the input- and coupler-bars.

Initially, I thought that the properties of a force-amplifying linkage, as discussed above, could be applied to provide the large forces necessary to break off coral lumps with the coral crushing apparatus of scarids. Dr J. L. van Leeuwen, however, convinced me that this cannot be the case. Although indeed the forces between the points P tend to infintity when the bars *a* and *d* are tending to the in-line position, the moment arms of these forces with respect to point Q tend to zero simultaneously! Using the formulae from Muller (1989), it can be proven that the moment in the limit case (i.e. when the bars *a* and *d* are in line) is equal to

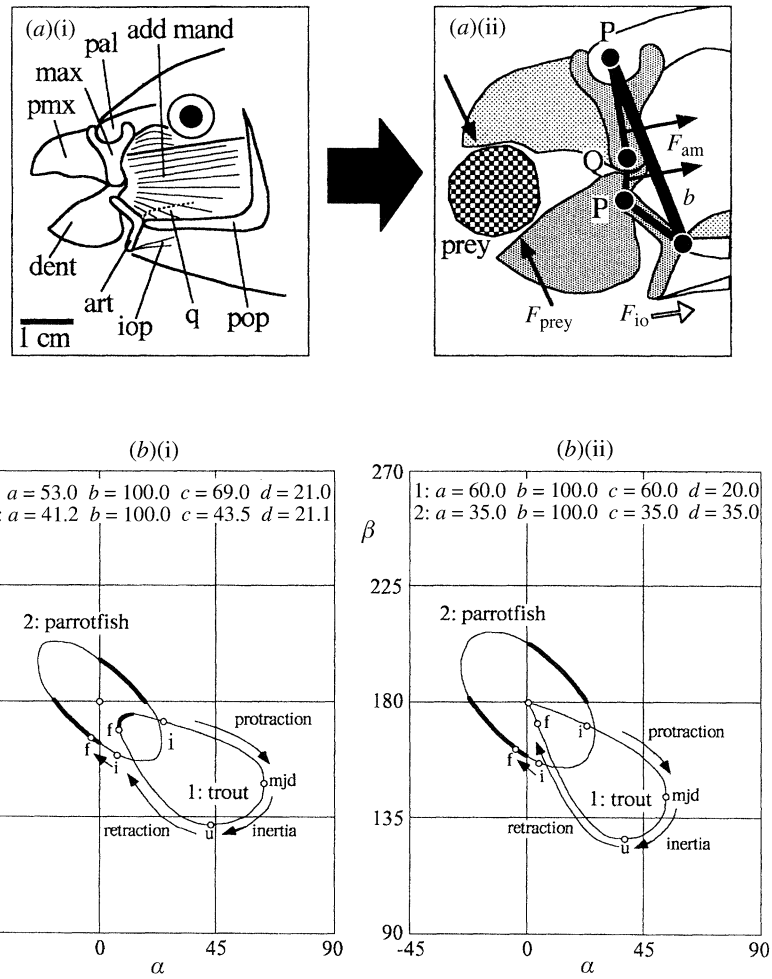

Figure 17. (*a*)(i)(ii) The (maxillare)-(lower jaw) linkage of the parrotfish, *Pseudoscarus forsteni* (modified after Van Dobben 1935) in a lateral view. The frame bar *b* is drawn bold. The anatomical names of the bars during biting are: *a* = maxillare, *b* = suspensorium, *c* = articulare, *d* = dentale. F_{am} = force exterted by adductor mandibulae muscle, F_{io} = force exterted by interopercular bone, F_{prey} = force exerted on prey. Normalized linkage dimensions are (*a*) : (*b*) : (*c*) : (*d*) = (41.2) : (100) : (43.5) : (21.1). These data were measured from stereo X-radiographs of the holotype. The linkage in diagram (*a*)(ii) is drawn in Van Dobben's picture and not entirely to scale. A 2T2l-linkage with transmission properties very close to the real linkage has dimensions (*a*) : (*b*) : (*c*) : (*d*) = (35.0) : (100) : (35.0) : (35.0). (*b*) Kinematic aspects of evolutionary transitions of (maxillare)-(lower jaw) system from a 'generalized' system as e.g. present in the trout (*Oncorhynchus*) to a 'specialized' system as found in *Pseudoscarus*. (*b*)(i) Using the real linkage dimensions; (*b*)(ii) using approximate function cognates. The folding properties of the (maxillare)-(lower jaw) linkage of the trout are lost in that of the parrotfish. i = initial position, mjd = maximal jaw depression, u = ultimate position, f = final position. See also figure 15. Further explanation in text (§6*b*).

$h.F_x$ (see figure 16*ci*). With the given geometry (figure 17*a*ii), this means that the fish cannot take any advantage of the large forces F_Y of figure 16*c*ii. So, Van Dobben (1935) was probably right when he wrote that the biting force in *Pseudoscarus* was approximately equal to the force exterted by the adductor mandibulae. The large pressures to break off coral lumps are possibly provided by the acute edges of the jaws.

In figure 17(*b*) the kinematic aspects of a transition from a 'generalized' (lower jaw)-(maxillare) system of e.g. a trout (*Oncorhynchus*; see above) to the 'specialized' mechanism of parrotfishes (*Pseudoscarus*) are shown (obviously, no taxonomic relationship between the two species is assumed to exist). This reveals not only a transformation from a folding '3Sopp(mlms)'-linkage to a non-folding '2T2l'-linkage, but also a limitation of the working range during action. It is also shown that the 'approximate function cognate' technique (§5*a*) gives a similar insight in this evolutionary change, using simpler linkages than the original ones.

(*c*) *Locking mechanisms and hysteresis*

Locking four-bar linkages are present in the neurocranium levation mechanism of some fishes (figures 18 19; Muller 1987). The system is particularly well developed in pipefishes (order *Gasterosteiformes*: several families: see Muller 1987; Altermatt 1991). It consists of: (i) the urohyal, sternohyoid, hypaxial muscle complex (*u*-bar); (ii) the pectoral girdle (*pg*-bar); (iii) the neurocranium, suspensorium complex (*n*-bar); and (iv) the hyoid (*h*-bar). Muller (1987) considered the system in an earth-bound frame. In this frame, the bar-sequence is: (*a*, *b*, *c*, *d*) ≡ (*u*, *pg*, *n*, *h*).

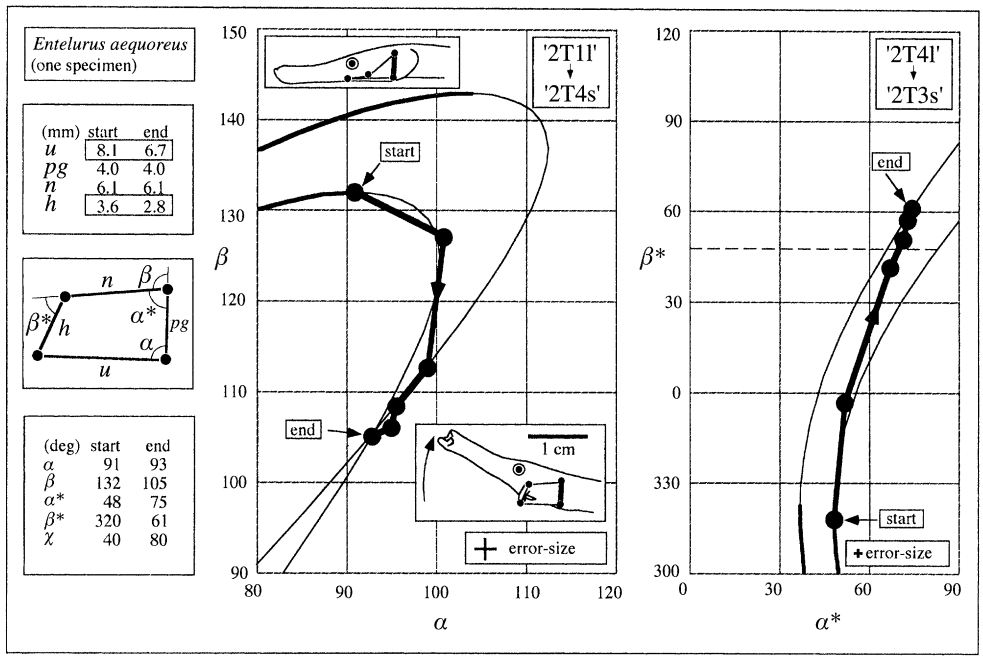

Figure 18. An example of hysteresis in a four-bar system of a feeding pipefish *Entelurus aequoreus* (head length = 25 mm), with and without taking shortening of the ventral head muscles and a correction for the projection of the hyoids into account. Left picture: transmission functions with bar *pg* as frame-link *b*. This picture gives the relation between the mouth bottom depression α and the neurocranium levation β (see Muller 1987). Right picture: transmission functions with bar *n* as frame-link *b*. Bar conventions and angles are as in figure 1. Anatomical abbreviations in Appendix 2.

Linkage dimensions and angles are indicated in the insets and were measured from a 400 fr s^{-1} movie with lateral and ventral views of the animal. α,β = in- and output angles of '2T1l'-'2T4s'-linkages, α^*,β^* = idem of '2T4l'-'2T3s'-linkages. The angle χ indicates the abduction angle between the two hyoid-bars. Time between subsequent points is 2.5 ms. The four-bar transmission curves were calculated with unshortened and maximally shortened bars, measured from the movie and from three-dimensional X-radiographs. The *u*-bar shortens through contraction of the sternohyoid and hypaxial muscles, the *h*-bar shortens by abduction of the hyoids. Note that abduction takes place immediately after the start of the movement (i.e. within 5 ms) and the system then behaves as a rigid one (with changed bar-lengths). Note also that it is not necessary that corresponding points lie at the same relative positions: e.g. the third data point in the left picture on the transmission curve and in the right one in between the transmission curves. This is due to the change of bar-lengths. Further explanation in text (§6*c*).

The neurocranium levation mechanism in syngnathids can be considered as a bistable system: at the start of the movement, suspensorium abduction and contraction of the sternohyoid and hypaxial muscles immediately occurs (within 5 ms). This results in the transformation of the original four-bar linkage ('2T1l') to another one in which the *u*- and *h*-bars differ from the original values ('2T4s'; see figure 18: left picture). The rest of the movement takes place along the transmission curve of the latter linkage. This transition is better shown in a fish-bound frame i.e. taking the *n*-bar as the frame. Then, the linkage is inversed from one (α,β) to another four-bar (α^*,β^*) linkage (figure 18: right picture). The bar-sequence becomes now: $(a, b, c, d) \equiv (pg, n, h, u)$. It is virtually impossible to obtain this insight into the functioning of the system by conventional frame-by-frame motion analysis.

Westneat (1990, 1994) extensively tested the motions of the four-bar linkages described above. He concluded that shortening of the bars during motion, as proposed by Muller (1987), gives good agreement between theoretical and measured positions. Altermatt (1991) tested the locking linkage in the snipefish, *Macrorhamphosus scolopax* and found excellent agreement between measured and predicted data.

As a conclusion, it is useful to apply planar four-bar system analysis to less rigid biological systems considering two extreme rigid linkages as limits for a region in which hysteresis (i.e. variability of a particular bar or its projection) occurs (figure 18). The question of the accuracy of such a system is discussed in §6*e*.

Muller (1987) considered the neurocranium levation mechanism in the shrimpfish, *Amphisile* as a 2-parameter 2T4s-linkage, to fit it in his one-parameter approach of these mechanisms. He argued that *Amphisile* minimizes its head movement (neurocranium levation: $\Delta\beta < 5°$). The transmission function with the real bar lengths (figure 19: curve no. 1) in *Amphisile* however does not resemble a 2T4s-linkage (figure 19: curve no. 2), but rather a 2T1l-one (figure 19: curve no. 3), because the *u*-bar (= *a*-bar) is extremely long. The real curve resembles also a 3Sadj(lmms) linkage (figure 10, top, right) but this representation misses the elegance of the reduction to a two-parameter system. The small working range implies that a distinguishment between a 2T- and a 3S-linkage is not needed. $\Delta\beta$

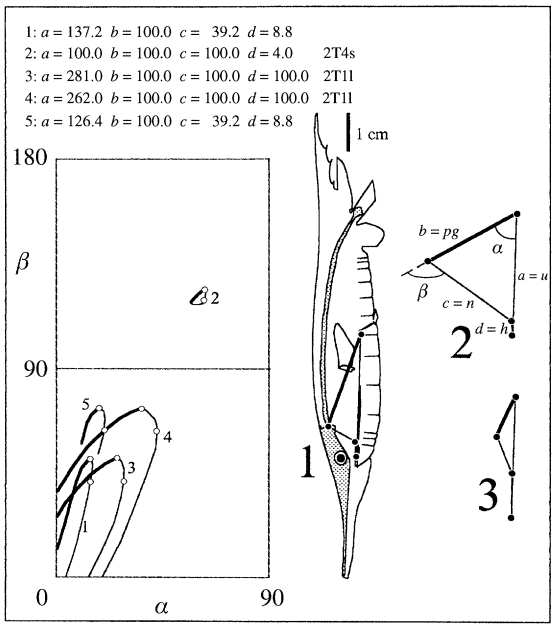

Figure 19. The neurocranium levation mechanism of the shrimpfish, *Amphisile sp.* 1: the real 4- parameter linkage; 2: considered as a 2T4s-linkage (Muller 1987); 3 and 4: considered as a 2T1l-linkage; 5: the real 4-parameter linkage with reduced *u*-bar. Bar-conventions and angles are as in figure 1. Anatomical abbreviations are in Appendix 2. The values for α_{locked} are for curve no. 1: 15°; for curve no. 2: 61°; for curve no. 3: 25°; for curve no. 4: 36° and for curve no. 5: 19°. Frame bars ($b = pg$) are drawn bold. Further explanation in text (§6*c*).

is now ca. 9° (measured from 1500 fr s^{-1} movies that we made), so the head movement in this fish is possibly not minimized as argued by Muller (1987). Note that there is still a difference in the α-range between curves 1 and 3.

A two-parameter simplification still appears to be valid because it satisfactorily predicts the actual neurocranium levation. Two interesting conclusions can be drawn: (i) hyoid length does only slightly influence neurocranium levation (compare in figure 19: slope and working range of curves no. 1 and 3), contrary to what one is tempted to think at first sight; and (ii) the output of the system is very sensitive to a change of the length of the *u*-bar (= bar *a*). A change of bar *a* from 281.0 to 300.0 (ca. 6.8%) makes system no. 3 in figure 19 non-functional. A similar change of bar *a* in the other direction, i.e. from 281.0 to 262.0 produces curve no. 4 in figure 19 which differs considerably from curve no. 3. Comparable results are obtained for the 4-parameter linkage: changing bar *a* from 137.2 to 148.0 (ca. 7.9%) makes the system non-functional. A change from 137.2 to 126.4 produces a transmission curve (no. 5: partly shown) rather different from curve no. 1.

The system may also be considered with the emphasis on the α-, β-, $\Delta\alpha$- and $\Delta\beta$-values. Curve no. 2 is invalid for all these four values. Curves no. 3 and 4 have about the same $\Delta\alpha$- and $\Delta\beta$-ranges but the absolute α- and β-values are very different. Curve no. 5 differs from curve no. 1 only in the absolute β-values. In the case of *Amphisile*, $\Delta\beta$ is the only important parameter but in other cases also the α-, β-, $\Delta\alpha$-values may have significance.

The above example illustrates also the valuability of the approximate function cognate approach: by simulating the system, using the real bar lengths, an approximate two-parameter linkage can be selected and so the system description adequately simplified (see §5*a*).

(*d*) *Cam mechanisms*

Cam mechanisms are found in e.g. a system formed by two joints (Alexander & Bennett 1987). Here, one of the links is substituted by two articulating surfaces, whereby the sum of the radii of curvature and distances is equal to the length of the 'missing link' (figure 20*a*, *b*). This bar is an 'imaginary bar'. The linkage in the hock of the sheep can be considered as a '2T4l'-linkage with two imaginary bars. In extreme extension and flexion (figure 20*b*), it reaches overlapping in-line positions (figure 2). Intermediate positions are reversely crossed (figure 2), so the system operates in the most non-linear part of the transmission-curve (figure 6). As the linkage is bistable (Alexander & Bennett 1987), a little strain of the ligament occurs during motion.

The structure of the cruciate ligament mechanism in the knee joint (figure 20*c*) lies in between a real four-bar linkage (all the bars are existing) and a cam-mechanism: the cruciate ligaments are kept taut by the cams formed by the femoral condyles and tibial articulating surface. This conversely crossed 2T4s-linkage (figure 2) also operates in the most non-linear part of the transmission curve (figure 6). In extreme extension and flexion, overlapping in-line positions are reached (figure 2; see Muller 1993*a*).

Badoux (1984) considered the cruciate ligament linkage in the knee joint of horse and dog as a straight line generator (Chebychev-type, see also Hartenberg & Denavit 1964; Dijksman 1976) which should adjust the instantaneous centre of rotation (ICR; see §2) of the knee joint during locomotion.

The shape of one of the articulating surfaces can be derived from the shape of the other one and the distance between the polode and the respective articulating surface (Straßer 1917; Huson 1974; Menschik 1974*a*). The position of the articulating surfaces is never at the polodes. So, the cruciate ligament four-bar linkage forces the articulating surfaces to roll and slide over each other (see §2). Implications of this fact for the mechanics of knee joints of different shape have been discussed by Muller (1993*b*). The dimensions of the cruciate ligament four-bar linkage limit the angle of rotation between femur and tibia (Muller 1993*b*) and determine the angles which the femoral and tibial axes make with the knee joint (Menschik 1974*a*; Muller 1993*a*). At the extreme positions of the cruciate ligament four-bar linkage, elasticity of the ligaments plays a role in limitation of the movement (see §6*c*). Badoux (1984) assumed a maximal strain of 6% for the cruciate ligaments, based on various references.

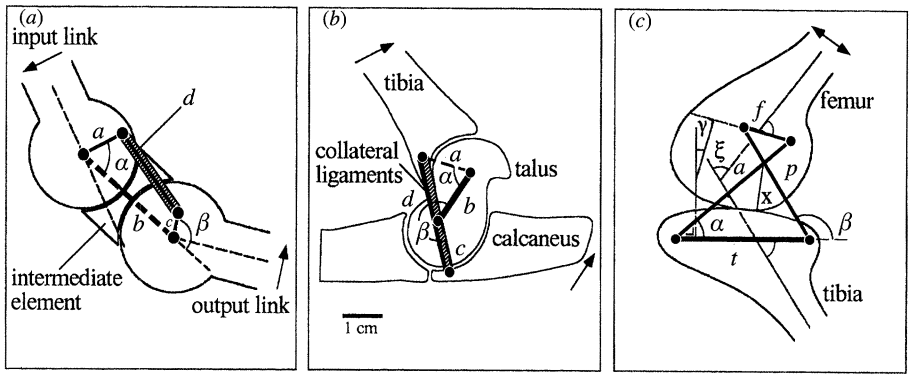

Figure 20. Examples of cam mechanisms. (*a*) General scheme of a two-joint linkage with a single ligament. Note that link *b* is not real (non-existing or imaginary). (*b*) An actual two-joint linkage in the hock of the sheep, *Ovis aries*. (*a*) and (*b*) modified after Alexander & Bennett 1987). Here, link *b* is on the intermediate element, so links *a* and *c* are imaginary. The linkage can be typified as a '2T4l'-linkage. (*c*) A diagram of the mammalian knee joint with the four-bar linkage in it (Muller 1993*b*). In this linkage, all bars are real, provided that the ligaments are kept taut. This can be considered as a '2T4s'-type linkage. Frame bars *b* are drawn bold. Anatomical abbreviations in Appendix 2.

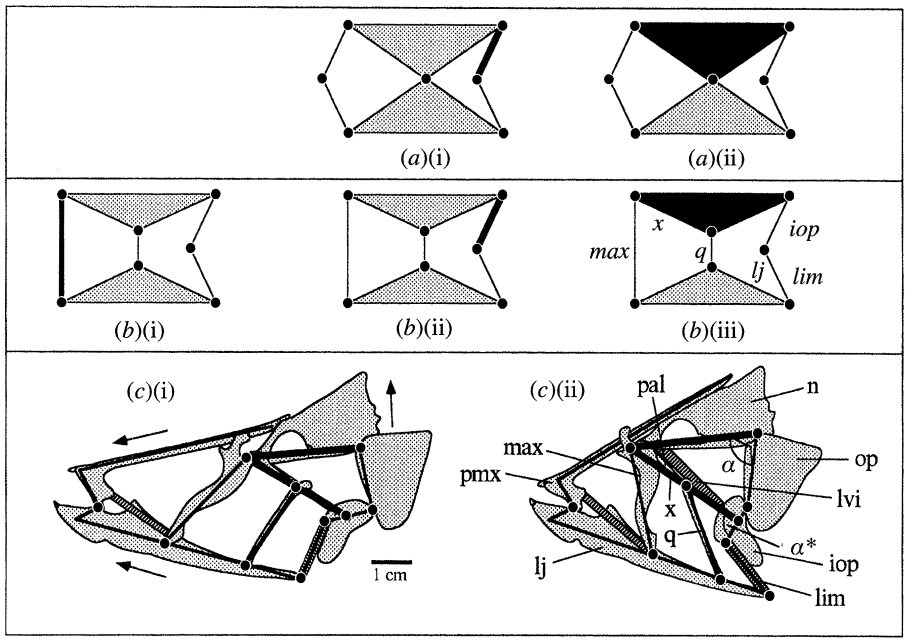

Figure 21. (*a*)(*b*) The five classes of planar constrained six-bar linkages (modified after Dijksman 1976) (*a*i) Watt-1 six bar; (*a*ii) Watt-2 six bar. (*b*i) Stephenson-1 six-bar; (*b*ii) Stephenson-2 six-bar; (*b*iii) Stephenson-3 six-bar. The four-and six-bar linkages in the sling-jaw wrasse, *Epibulus insidiator* (redrawn after Westneat & Wainwright 1989). The rest situation of *Epibulus* is drawn right (*c*ii) for comparison with the corresponding Stephenson-3-mechanism that is protruded (*c*i). Frame bars *b* are drawn bold. The main elements of the four-bar linkage that drives the six-bar linkage are: *a* = operculum, *b* = neurocranium, *c* = vomero-interopercular ligament, *d* = interoperculum. The six-bar linkage is in fact composed of a five- and a four-bar linkage (§6*e*). The interoperculum is the input-bar of the six-bar linkage, the vomero-interopercular ligament is the frame-bar. Output-bars are the maxillare and the quadratum. Coupler-bars are the lower jaw and the interoperculo-mandibular ligament. Anatomical abbreviations in Appendix 2. *x* = vomero-interopercular ligament-bar.

(*e*) *Coupled linkages and four-bar replacement mechanisms*

Five different types of six-bar constrained linkages exist belonging to two different classes: Watt- and Stephenson-mechanisms (figure 21). These linkages have a mobility 1 (Dijksman 1976). A Watt linkage can be considered as a four-bar linkage connected to another four-bar linkage, a Stephenson linkage as a four-bar linkage connected to a five-bar linkage. It can be easily verified that the combination of the opercular- and jaw- four-bar linkages in *Cheilinus* (figure 14*a*ii,iii) can be considered as a Watt-2 six-bar linkage (figure 21*a*ii).

The only example of a Stephenson six-bar linkage known in biology is the snout protrusion mechanism found in the head of the extremely evolved labrid fish *Epibulus insidiator* ('sling-jaw wrasse', Westneat & Wainwright 1989; Westneat 1991). This linkage is of the Stephenson-3 type (figure 21). During snout

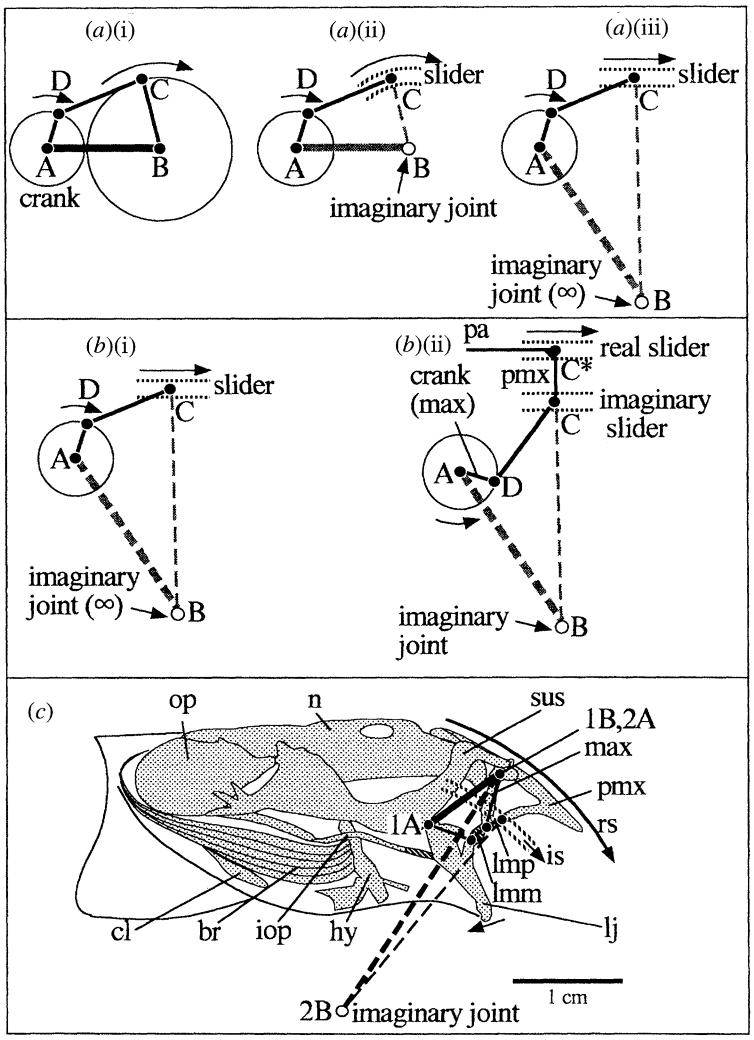

Figure 22. Examples of crank-slider linkages. (*a*) Derivation of crank-slider linkage from a four-bar linkage. (*b*) Definition of real and imaginary sliders (pictures *b*i and *a*iii are the same). (*c*) Jaw protrusion mechanism in the dragonet, *Callionymus lyra*, formed of a crank-slider linkage driven by a four-bar linkage (modified after Kayser 1961). The four-bar linkage is equivalent with the maxillare-system in the trout (§6*b*), the crank-slider linkage is equivalent with picture (*b*)(ii). Frame bars *b* are drawn bold. Anatomical abbreviations in Appendix 2. rs = real slider, is = imaginary slider.

protrusion it is driven by a modified opercular four-bar linkage (compare §6*a*).

Westneat (1991) has proposed evolutionary changes in the feeding mechanisms of the fishes in the *Cheilinid-Epibulus* transition. He argues that at a particular stage, two bars (parameters) should change simultaneously (i.e. loss of the palatine link and gain of the quadrate link). Although I agree with his statement that: '... the most parsimonious is one that combines the fewest number of evolutionary events into a biomechanically feasible series of intermediate forms...', it is a question of what is still biomechanically feasible! The movement-possibilities of the linkage are extremely sensitive to e.g. a small change in length of the quadratum (ca. 5% change makes the system non-functional). As the mechanical behaviour of a linkage in fact is undetermined by simultaneous alteration of two bars (see §5*c*, table 5) and as the direction of evolution is *a priori* unknown, it is in my view very unlikely that such a transition could occur. So, I think that other evolutionary pathways have to be searched for. For example, when *Epibulus* would have been evolved directly from an ancestor possessing the more generalized maxillare-(lower jaw) linkage in teleosts (see §6*b*, figure 15), the problem of loss of the palatinal joint would not be present. The occurence of a (small) ligamentum maxillo-mandibulare does not impede the development of a movable quadrate link. As at present solid information about the evolution of *Epibulus* is lacking, the above and other possible suggestions remain rather speculative.

In the protrusion apparatus of the jaws of teleost fishes (Alexander 1967; Motta 1984), a so-called 'crank-slider' mechanism is often found. A crank-slider linkage can be derived from an ordinary four-bar linkage by replacing the output link (bar *c*) by a slider connected to the frame bar *b* (figure 22*a*; see also Hartenberg & Denavit 1964: §2.15). The radius of curvature of the slider is equal to the length of bar *c*. Moving point B to a large distance results in a straight

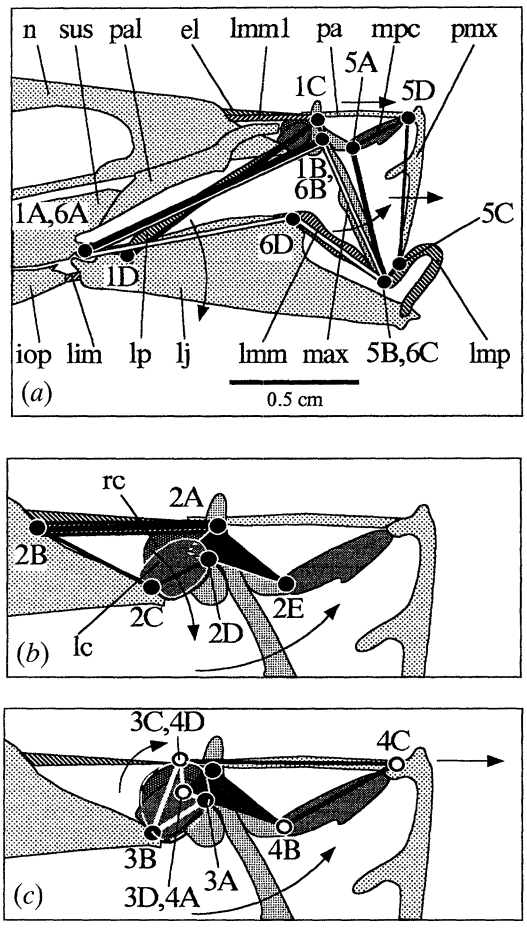

Figure 23. The highly complex jaw protrusion mechanism in the sand-eel, *Ammodytes tobianus* (modified after Kayser 1961), consisting of 2 × 6 coupled four-bar linkages. Anatomical abbreviations in Appendix 2. (*a*) Overview of whole jaw apparatus. the maxillare has five processes: lateral (the longest one), premaxillary (rostral), dorsal, cranial (caudal) and medial (not shown). The rostral processus of the palatinum proceeds to the dorsal processus of the maxillare. (*b*)(*c*) Details. The joints 1B, 2D and 3A are the same. Four-bar linkage no. 3 is indicated with white bars. Four-bar linkage no. 4 is indicated with white dots at the joints.

The anatomical structures which form the bars

linkage no.	*a*	*b*	*c*	*d*
1	*lj*	see below [a]	*max*	*lp*
2	*max*	*lmm*1	*n*	*lc*
3	*max*	*lc*	*rc*	*lig. rc-max*
4	*lig. rc-max*	*max*	*mpc*	*pa*
5	*mpc*	*max*	*lmp*	*pmx*
6	*lj*	see below [a]	*max*	*lmm*

[a] This 'bar' is formed by the virtually constant distance between the quadrato-articular joint and the pivot of the maxillary.

slider (figure 22*a*iii). Crank-slider linkages can only be typified by 2-parameter four-bar linkages when bars *b* and *c* are not too long compared to the coupler and the crank (as e.g. in figure 22*a*ii).

Curved sliders are found e.g. in *Callionymidae*. In other teleosts, the slider may be more or less straight or even (slightly) inversely curved, as is the case in *Epibulus* (figure 21). The point B is eliminated to become an 'imaginary joint'. In the dragonet, *Callionymus*, and in 'generalized' teleosts, the crank-slider linkage for premaxillary protrusion is driven by the four-bar linkage that causes rotation of the maxillare (see §6*b*, figure 15). A peculiarity of the protrusion mechanism in fish is that the place of the morphological slider does not coincide with the theoretical slider place of the crank-slider chain. This is explained in figure 22*b*. In diagram 22*b*i, a conventional crank-slider linkage is drawn. Diagram 22*b*ii differs from 22*b*i in two respects. First, the direction of rotation of the crank is reversed. Second, the slider is modified: the 'processus ascendens' (pa) of the 'premaxillare' (pmx) moves over a really existing slider (C*). The original slider (C) may exist or not. In the latter case, we may speak of an 'imaginary slider'. In the actual system, confusion of real and imaginary sliders may result in an erroneous position of point C and so in a wrong dimensioning of the linkage. Additionally, a morphological base for a choice of point C on the real slider (i.e. the processus ascendens) lacks. Figure 22*c* shows the actual situation in *Callionymus lyra*. In *Epibulus* (figure 21), the maxillare (connected to the six-bar linkage) can be considered as crank, part of the lower jaw as coupler link, the point of connection between lower jaw and premaxillare as imaginary slider point and the processus ascendens of the premaxillare as real slider.

The protrusion mechanism found in the sand eel, *Ammodytes tobianus* (figure 23, Kayser 1961) is the most complex coupled biological linkage known to M.M. It is not a crank-slider mechanism as in generalized teleosts (see above), but it consists of a bilateral series of six four-bar linkages.

The movement during prey capture proceeds as follows (figure 23; Kayser 1961: figures 8, 18). Initially, the mouth opens by depression of the lower jaw. The slider-like coronoid process of the lower jaw pushes the maxillare forward. At a larger lower jaw depression the contact between the coronoid process and the maxillare is lost. Now, the maxillare is rotated forward by the four-bar linkages nrs. 6, and later 1 in figure 23*a*. Linkage 6 is equivalent with the system described for the trout (§6*b*). A difference with the trout-system is that the ligamentum maxillo-mandibulare is relatively long and partly cartilaginous and so it can push the maxillare (Kayser 1961: p. 369). Force transmission to the maxillare is zero in a completely folded position of linkage 6 and begins to play a role when this linkage is brought to its workable initial position (see above). Figure 23*a* reveals that linkages nrs. 1 and 6 in fact would form a non-movable system when the bars would be all rigid. However, one of the 'bars' of linkage no. 1 is the ligamentum primordiale (figure 23*a*: *lp*) which becomes taut close to the ultimate position of the maxillare (figure 23*c*). So, linkage 1 'helps' linkage 6 when the kinematic transmission of the lower jaw (linkage 6: α) to the maxillare (linkage 6: β) tends to become too weak, i.e. when in linkage 6, β becomes rather constant (figure 24: left diagram).

The premaxillare is at two points pushed forward by four-bar linkage no. 5 (figure 23*a*). The ligamentum

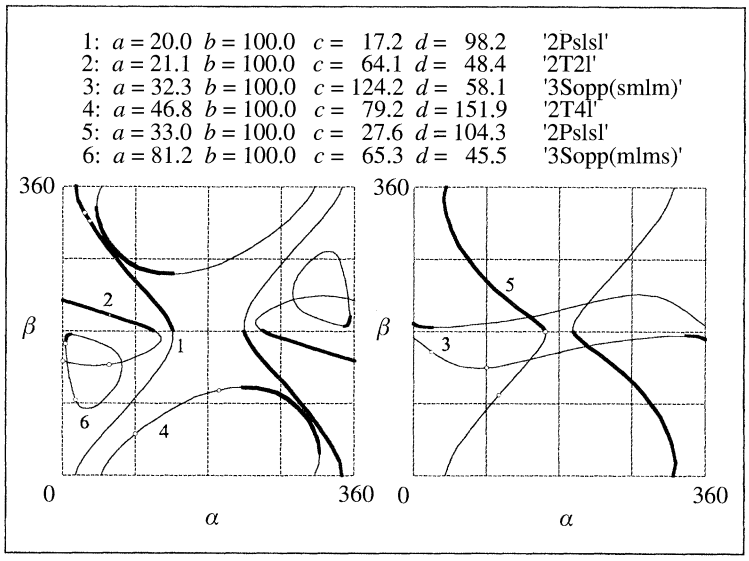

Figure 24. Transmission curves of linkages drawn in figure 23. Bold lines: crossed configurations, thin lines: uncrossed configurations. $\alpha_i,\beta_i = \alpha,\beta$ in initial position, $\alpha_f,\beta_f = \alpha,\beta$ in final position.

The approximate working ranges (in degrees)

(Values between parentheses are represented in the diagrams. Although measured as accurate as possible, using preserved animals as well as a mechanical model, these values have to be considered with caution. A more rigorous study is needed to improve the table.)

linkage no.	α_i	β_i	α_f	β_f
1	25–30	330–322	30–35	322–314
2	ca. 0	ca. 150	60–70	ca. 150
3	80–100 (90)	ca. 145	20–30	150–160
4	200–210 (from model)	ca. 100	60–120 (90)	ca. 50
5	→ 180–200	→ 180	110–120	110–120
6	→ 0	→ 180	18	94

maxillo-premaxillare (figure 23*a*: lmp) is rather solid between points 5B and 5C (figure 23*a*) and so can act as a rigid link. It is probably loaded in a compressive as well as in a tensile way during protrusion and so needs a small amount of play.

The position and movement of the pivot of the maxillare (figure 23*b*: point 2D) is controlled by four-bar linkage no. 2 in figure 23*b*. The mesethmo-maxillar ligament (figure 23*a*: lmml) has to remain continuously taut. To prevent dorsocaudally tilting of the whole protrusion system, linkage no. 2 is supported by the palatinum when the mesethmo-maxillar ligament would be compressed.

The movement of the processus ascendens of the premaxillare is at both ends controlled by four-bar linkage no. 4 in figure 23*c*. This linkage is also driven by linkage no. 3 in figure 23*c*. So, the movement of the premaxillare is controlled in 3 points at each side. The elastic ligament limits the protrusion at its final position.

Figure 24 gives the transmission functions and working ranges of the four-bar linkages of figure 23. It is interesting that very different properties of several types of linkages have been merged in evolution. Two parallellogram-like linkages are present (nrs. 1 and 5), one operating in a reversely crossed configuration, the other starts at the transition of crossed and non-crossed configurations. One of the two trapezoidal linkages (no. 2) possesses an approximately constant β-range, where α varies considerably. This means that bar *a* may rotate over a large angle whereas the other bars are rather stationary. This allows a free suspension of the pivot of the maxillare, without a direct coupling to the neurocranium (ethmoid) as is the case in generalized teleosts. The other trapezoidal linkage (no. 4) makes use of the non-linear transmission function. It starts almost from a locked position. The remaining linkages (nrs. 3 and 6) are close to 3Sopp-linkages. They operate in reversely folding configurations (figure 2, §2).

Four-bar analysis of such a complex system of linkages is of considerable help in the investigation of its movement-possibilities and working ranges and so confers better insight into the mechanics than could be (or was!) obtained by conventional morphological examination (Kayser 1961 and references therein). It may give insight into where ligaments and bony (cartilaginous) elements are required and where rigid and slackening, elastical or limiting structures are necessary. It also provides a powerful check on the validity of the mechanical consideration because mechanical feasibility, transmission functions and working ranges have to fit in which each other. These features are greatly influenced by slight changes in the

four-bar linkages. For example, a small (e.g. 5%) change of a bar of linkage no. 6 destroys its folding properties (see also table 5). This means that the mouth cannot be closed anymore and so the whole protrusion system is jammed.

The small range of a crossed configuration in figure 24: curve 6 is removed when the linkage is in the range of relevant positions (i.e. close to folding; compare figures 15 and 17). So, curve 6 demonstrates the sensitivity of the linkage for small changes of bars. Such 'artifacts' have to be eliminated in the working system, e.g. by 'play' in the joints (see below).

The constrained linkage-system in *Ammodytes tobianus* has still a mobility 1. Dijksman & Timmermans (1994) have studied possibilities for the design of multi-bar linkages with mobility 1, especially so-called 'prime-chains'. This theory may possibly be of help in future studies of complex mechanisms in animals.

The very complex structure of coupled linkages in biological systems, as discussed above, addresses the question about the functional range of necessary and undesired hysteresis. In *Ammodytes tobianus*, the protrusion mechanism of the jaws consists of 2×6 coupled four-bar linkages. This mechanism is very sensitive to changes in bar-lengths. As biological structures have no mathematical accuracy, a smoothly functioning system requires a certain amount of hysteresis or 'play' (see §5*a*, 6*c*, *d*). Too much hysteresis will make the system non-functional. It is interesting to investigate the allowable deviations of the system in question and so the required accuracy during its evolution. This has not been carried out hitherto. Table 5 and §5*d* may be very heplful in such studies.

7. DISCUSSION

Within the application of four-bar linkage theory in biological systems the emphasis of previous studies has been quite various as shown in the following list.

1. Determination of degrees of freedom and physical constraints (Alexander 1967, 1983; Elshoud 1986; Alexander & Bennett 1987).

2. Determination and application of kinematic and dynamic (force) transmission (Frazzetta 1962; Bock 1964; Alexander 1967, 1973; Liem 1970; Iordanski 1971; Anker 1974; Barel *et al.* 1975, 1977; Aerts & Verraes 1984; Muller 1987, 1989; Aerts 1991; Westneat 1991).

3. Derivation of coupler plane curves for a particular motion (Badoux 1984). A special type of such curves (Burmester-curves, see Burmester, 1888) has been extensively discussed by Menschik (1974*b*) and Müller (1983). The latter two papers were heavily criticized by Fuss (1991).

4. Derivation of velocity pole curves and profile shapes in the coupler plane (Huson 1974; Menschik 1974*a*). These studies aim to construct condylar fitting surfaces from the polodes.

5. Derivation of limitations for movement possibilities (Menschik 1974*a*; Alexander & Bennett 1987; Muller 1993*a*, *b*).

6. Optimization of artificial four-bar prostheses (many papers, e.g. Hobson & Torfason 1974, 1975).

The above-mentioned approaches study aspects of linkage functioning in rather specific systems or situations. This approach however, aims to place the different linkages in a general framework. Such an overview gives insight in the mechanical suitability of particular linkage functions for particular purposes, in evolutionary possibilities, in the effectiveness of a particular composition of linkages in complex biological systems, in the available freedom to obtain mechanically feasible constructions. Additionally, it provides a powerful method to validate or falsify a particular mechanical approach for a biological system (see §6*e*). Another advantage is that it enables thinking about the mechanical functioning of biological systems without requiring knowledge of mathematics. This makes it also very suitable for educational purposes. Obviously, four-bar theory offers also many possibilities for more mathematically oriented studies (Aerts & Verraes (1984) and many engineering texts). The consideration of linkage mechanics in the present paper and in the references mentioned is always time-independent. Introduction of a time-dependent aspect is technically possible but mostly gives rise to rather complex differential equations.

An interesting aspect is whether linkage theory may help to discover a possible 'optimal design' of a structure. Optimization may take place following the transmission function of a single linkage, or via transitions to other linkages. Table 5 shows that there are many ways to derive a particular linkage with its (part of) a particular transmission function from other linkages. It is tempting to think that evolutionary pathways have to follow the principle of 'minimal redundancy' implying that evolution has to take place along a path with the minimal amount of transitions, and so the minimal amount of 'problems'. The more transitions are present, the greater is the chance that a non-functional situation or a barrier is met, or possibilities for an evolutionary change become too small. The question of simultaneous changes of parameters has already been discussed in §6*e* . In the same section, it has been argued that there is a limited range of allowable hysteresis in many complex biological systems. Therefore it is also interesting to study how linkage functioning is maintained and possibly changed during allometric growth.

It is apparent, especially from the examples discussed in §6*e* (*Epibulus*, *Callionymus*, *Ammodytes*) that it is very difficult, or even impossible, to generate compound systems of biological linkages via a completely deductive way, i.e. from functional demands and physical principles only. Information about the basic composition of the system is needed *a priori* to understand the functioning of the structure.

Finally, it should be realized that many linkages are in fact three-dimensional (see Wismans *et al.* 1980; Otten 1983; Elshoud 1986; Van Gennip 1988; Aerts 1991). As in a three-dimensional model the large amount of movement-possibilities and parameters rapidly may lead to a loss of survey, it is useful to investigate whether two-dimensional approaches may give insight in aspects of functioning. Although a simple model often does not closely represent the real

structure and its simplifying approximations make it often rather vulnerable, it has also explanatory power. An example are the knee joint models (Huson 1974; Menschik 1974*a*). It is very difficult to predict real condylar shapes with these models but they provide a useful tool for thinking about construction principles for inarticular joints (Alexander & Bennett 1987; Müller 1983; Muller 1993*a*, *b*).

I thank Dr E. A. Dijksman, Dr P. Aerts, Professor R. McN. Alexander and Dr Ir J. L. van Leeuwen for comments on the manuscript, Dr E. A. Dijksman for tuition on kinematic engineering and Ir M. H. E. de Lussanet for many stimulating discussions and useful comments. Mr A. Terlouw helped with X-radiography and with the analysis of the *Amphisile*-system and Dr M. J. P. van Oijen kindly lent some fish specimens for anatomical study. Mr W. Valen carefully made many of the 'difficult' illustrations and Professor Dr J. W. M. Osse provided a photograph of a *Latimeria* skeleton.

REFERENCES

Aerts, P. 1991 Hyoid morphology and movements relative to abducting forces during feeding in *Astatotilapia elegans* (*Teleostei: Cichlidae*). *J. Morph.* **208**, 323–345.

Aerts, P. & Verraes, W. 1984 Theoretical analysis of a planar four-bar linkage in the teleostean skull. The use of mathematics in biomechanics. *Annals Soc. r. zool. Belg.* **114**, 273–290.

Aerts, P. & Verraes, W. 1987 Do inertial effects explain the maximal rotation of the maxilla in the rainbow trout (*Salmo gairdneri*) during feeding? *Annals Soc. r. zool. Belg.* T.**117**, fasc. 2: 221–235.

Alexander, R. M. 1967 Mechanics of the jaws of some atheriniform fish. *J. Zool.* **151**, 233–255.

Alexander, R. M. 1973 Jaw mechanisms of the coelacanth *Latimeria*. *Copeia* pp. 156–158.

Alexander, R. M. 1982 *Optima for animals*. London: Edward Arnold.

Alexander, R. M. 1983 *Animal mechanics*, edn 2. Oxford: Blackwell Scientific Publications.

Alexander, R. M. & Dimery, N. J. 1985 The significance of sesamoids and retro-articular processes for the mechanics of joints. *J. Zool. Lond.* A **205**, 357–371.

Alexander, R. M. & Bennett, M. B. 1987 Some principles of ligament function, with examples from the tarsal joints of the sheep (*Ovis aries*). *J. Zool., Lond.* **211**, 487–504.

Altermatt, R. U. 1991 Zur Kopfanatomie des Schnepfenfisches, *Macrorhamphosus scolopax* (*Teleostei, Syngnathiformes*). Inaugural Dissertation. Universität Basel. Schlattman. (In German.)

Anker, G. Ch. 1974 Morphology and kinetics of the stickleback, *Gasterosteus aculeatus*. *Trans. zool. Soc. Lond.* **32**, 311–416.

Badoux, D. M. 1975 General biostatics and biomechanics. In *Anatomy of the domestic animals* (ed. R. Getty), vol. 1, edn 5, chapt. 5, pp. 58–83. London: Saunders.

Badoux, D. M. 1984 The geometry of the cruciate ligaments in the canine and equine knee joint, a Tchebychev mechanism. *Acta anat.* **119**, 60–64.

Barel, C. D. N., Berkhoudt, H. & Anker, G. Ch. 1975 Functional aspects of four-bar systems as models for mouth opening mechanisms in teleost fishes. *Acta Morph. Neerl-Scand.* **13**, 228–229.

Barel, C. D. N., Van der Meulen, J. W. & Berkhoudt, H. 1977 Kinematischer Transmissionskoeffizient und Vierstangensystem als Funktionsparameter und Formmodel für Mandibuläre Depressionsapparate bei Teleostiern. *Anat. Anz.* **142**, 21–31. (In German.)

Barker, C. R. 1985 A complete classification of planar four-bar linkages. *Mech. Machine Theor.* **20**, 535–554.

Bock, W. J. 1964 Kinetics of the avian skull. *J. Morph.* **114**, 1–42.

Burmester L. 1888 *Lehrbuch der Kinematik*. Leipzig, Germany: A. Felix Verlag. (In German.)

Dijksman, E. A. 1975 How to design four-bar function cognates. *I. Mech. E.* 847–853.

Dijksman, E. A. 1976 *Motion geometry of mechanisms*. Cambridge University Press.

Dijksman, E. A. & Timmermans, E. A. 1994 Look-out for prime-chains with a prescribed number of mobility-degrees of freedom. Type synthesis of prime-chains. *Mech. Mach. Theor.* **29**, 653–672.

Elshoud, G. C. A. 1986 Fish and chips. Computer models and functional morphology of fishes. PhD thesis Rijksuniversiteit Leiden.

Fichter, E. F. & Hunt, K. H. 1979 The variety, cognate relationships, class and degeneration of the coupler curves of the planar 4R linkage. *Proceedings of the 5th world congress on theory of machines and mechanisms*, pp. 1028–1031.

Frazzetta, T. H. 1962 A functional consideration of cranial kinesis in lizards. *J. Morph.* **111**, 287–296.

Frazzetta, T. H. 1966 Studies on the morphology and function of the skull in *Boidae* (*Serpentes*). Part II. Morphology and function of the jaw apparatus in *Python sebae* and *Python molurus*. *J. Morph.* **118**, 217–296.

Fuss, F. K. 1991 Biometrics of the four-bar link of the cruciate ligaments in projection on the flexion-extension plane of the human knee joint. *Anat. Anz. Jena* **173**, 51–59.

Greene, M. P. 1983 Four-bar linkage knee analysis. *Orthop. Prosthet.* **37**, 15–24.

Hain, K. 1964 Das Spektrum des Gelenkvierecks bei veränderlicher Gestell-Länge. *Forsch. Ing.-Wes.* **30**, 33–64. (In German.)

Hartenberg, R. S. & Denavit, J. 1964 *Kinematic synthesis of linkages*. New York: McGraw-Hill Inc.

Hobson, D. A. & Torfason, L. E. 1974 Optimization of four-bar knee mechanisms: a computerized approach. *J. Biomech.* **7**, 371–376.

Hobson, D. A. & Torfason, L. E. 1975 Computer optimization of polycentric prosthetic knee mechanisms. *Bull. Prosth. Res.* **Spring 1975**, 187–201.

Hunt, K. H. 1978 *Kinematic geometry of mechanisms*. Oxford: Clarendon Press.

Huson, A. 1974 Biomechanische Probleme des Kniegelenks. *Orthopäde* **3**, 119–126. (In German.)

Iordanski, N. N. 1971 A contribution to the functional analysis of the skull in lizards (*Lacertidae*). *Zoologiceskij Zurnal.* **50**, 724–733 (In Russian.)

Kayser, H. 1961 Der Bau und die Funktion des Kiefer- und Kiemenapparates von Knochenfischen der Gattungen *Ammodytes* und *Callionymus*. Zool. Beiträge. *Neue Folge. Band* **7**, Drittes Heft. 321–445. Berlin: Duncker & Humblot. (In German.)

Liem, K. F. 1970 Comparative functional anatomy of the *Nandidae* (*Pisces, Teleostei*). *Fieldiana, Zool.* **56**, 1–166.

Menschik, A. 1974*a* Mechanik des Kniegelenkes. *Teil 1. Z. Orthop.* **112**, 481–495. (In German.)

Menschik, A. 1974*b* Mechanik des Kniegelenkes. *Teil 3.* Wien: Sailer. (In German.)

Moolenaar, G. J. 1983 Kinematics of the reciprocal apparatus in the horse. *Zbl. Vet. C. Anat. Histol. Embryol.* **12**, 278–287.

Motta, P. J. 1984 Mechanics and function of jaw protrusion in teleost fishes: a review. *Copeia* **1**, 1–18.

Muller, M. 1987 Optimization principles applied to the mechanism of neurocranium levation and mouth bottom depression in bony fishes (*Halecostomi*). *J. theor. Biol.* **126**, 343–368.

Muller, M. 1989 A quantitative theory of expected volume changes of the mouth during feeding in teleost fishes. *J. Zool.* **217**, 639–661.

Muller, M. 1993*a* The angles of femoral and tibial axes with respect to the cruciate ligament four-bar system in the knee joint. *J. theor. Biol.* **161**, 221–230.

Muller, M. 1993*b* The relationship between the rotation possibilities between femur and tibia and the lengths of the cruciate ligaments. *J. theor. Biol.* **161**, 199–220.

Müller, W. 1983 The knee. Form, function, and ligament reconstruction. Springer Verlag. Berlin. (In German.)

Nash, W. A. 1977 *Strength of materials. Schaum's outline series*, 2nd edn. New York: McGraw-Hill.

Osse, J. W. M. 1983 Morphology and evolution. *Acta Morphol. Neerl.-Scand.* **21**, 49–67.

Otten, E. 1983 The jaw mechanism during growth of a generalized *Haplochromis* species: *H. elegans* Trewavas 1933 (*Pisces, Cichlidae*). *Neth. J. Zool.* **33**, 55–98.

Reuleaux, F. 1876 *The kinematics of machinery. Outlines of a theory of machines*. New York: Dover Publications Inc. (Reprinted 1983.)

Straßer, H. 1917 *Lehrbuch der Gelenkmechanik. III Band: Spezieller Teil. Die untere Extremität*. Berlin: Julius Springer. (In German.)

Thomson, A. J. & Thompson, W. A. 1977 Dynamics of a bistable system: the click mechanism in dipteran flight. *Acta Biotheor.* **26**, 19–29.

Van Dobben, W. H. 1935 Über den Kiefermechanismus der Knochenfische. Extrait des archives Néerlandaises de zoologie. Tome II, 1e livraison: 1–72. (In German.)

Van Gennip, E. M. S. J. 1988 A functional morphological study of the feeding system in pigeons (*Columba livia L.*). PhD thesis Rijksuniversiteit Leiden.

Westneat, M. W. 1990 Feeding mechanics of teleost fishes (*Labridae*): A test of four-bar linkage models. *J. Morph.* **205**, 269–295.

Westneat, M. W. 1991 Linkage biomechanics and evolution of the unique feeding mechanism of *Epibulus insidiator* (*Labridae: Teleostei*). *J. exp. Biol.* **159**, 165–184.

Westneat, M. W. 1994 Transmission of force and velocity in the feeding mechanisms of labrid fishes (*Teleostei, Perciformes*). *Zoomorphology* **114**, 103–118.

Westneat, M. W. & Wainwright, P. C. 1989 The feeding mechanism of *Epibulus insidiator*: evolution of a novel functional system. *J. Morph.* **202**, 129–150.

Wismans, J., Veldpaus, F., Janssen, J., Huson, A. & Struben, P. 1980 A three-dimensional mathematical model of the knee joint. *J. Biomech.* **13**, 677–685.

Received 6 April 1995; accepted 19 July 1995

APPENDIX 1

List of abbreviations used in text and figures

a	= input link of four-bar linkage (figure 1)
A	= coordinates of joint between bar a and bar b of four-bar linkage (figure 1)
adj	= adjacent
b	= frame link of four-bar linkage (figure 1)
B	= coordinates of joint between bar b and bar c of four-bar linkage (figure 1)
c	= output link of four-bar linkage (figure 1)
c	= crank = revolving bar of four-bar linkage
C	= coordinates of joint between bar c and bar d of four-bar linkage (figure 1)
d	= coupler link of four-bar linkage (figure 1)
D	= coordinates of joint between bar d and bar a of four-bar linkage (figure 1)
F	= force (with subscripts)
F_{am}	= force exterted by adductor mandibulae muscle (figure 17)
F_{io}	= force exterted by interopercular bone (figure 17)
F_p	= force exerted on prey (figure 17)
F_x	= force in x-direction (figure 17)
F_y	= force in y-direction (figure 17)
ICR	= instantaneous centre of rotation (figure 1)
opp	= opposite
r	= rocker = oscillating bar of four-bar linkage
x	= x coordinate
y	= y coordinate
α	= input (interior) angle of four-bar linkage, between bar a and bar b (figure 1)
β	= output (exterior) angle of four-bar linkage, between bar b and bar c (figure 1)
β_a	= abduction angle of jaws (figure 16)
γ	= angle between perpendiculars on f and t, $\gamma = 0°$: 'straight leg' (figure 20)
χ	= abduction angle of hyoids in locked linkage of pipefishes (figure 18)
ξ	= angle between femoral and tibial axes ($\xi = 0°$ for leg straight) (figure 20)

APPENDIX 2

List of abbreviated biological structures

a	= anterior cruciate ligament (bar) (figure 20)
add mand	= adductor mandibulae muscle (figure 17)
art	= articulare (figure 17)
br	= branchiostegal rays (figure 15, 22)
cal	= calcaneus (figure 14)
cl	= cleithrum (figure 22)
dent	= dentale (figure 17)
el	= elastic ligament (figure 23)
f	= femoral distance between points of attach of cruciate ligaments (figure 20)
fem	= femur (figure 14)
gas	= gastrocnemius (figure 14)
h	= hyoid (bar) (figure 16, 18, 19)
hy	= hyoid (figure 22)
ih	= interhyale (figure 14)
iop	= interoperculum (figure 15, 17, 21, 22, 23)
j	= jaw-suspensorium-bar (figure 16)
lim	= interoperculo-mandibular ligament (figure 15, 21, 23)
lj	= lower jaw (figure 15, 21, 22, 23)
lmm	= maxillo-mandibular ligament (figure 15, 22)
lmm1	= mesethmo-maxillar ligament (figure 23)
lmp	= maxillo-premaxillar ligament (figure 22, 23)
lp	= primordial ligament (figure 23)
lvi	= vomero-interopercular ligament (figure 21)
max	= maxillare (figure 15, 17, 21, 22, 23)

met = some metatarsal bones (figure 14)
mpc = maxillo-premaxillar cartilage (figure 23)
muz = muzzle unit (figure 14)
n = neurocranium (bar) (figure 15, 18, 19, 21, 22, 23)
na = anterior part of neurocranium (figure 14)
np = posterior part of neurocranium (figure 14)
op = operculum (figure 15, 21, 22)
p = posterior cruciate ligament (bar) (figure 20)
pa = processus ascendens of premaxillare (figure 22, 23)
pal = palatinum (figure 14,17,21)
par = parasphenoid (figure 15)
pg = pectoral girdle (bar) (figure 18, 19)
pmx = premaxillare (figure 15, 17, 21, 22, 23)
pop = preoperculum (figure 17)
pter = pterygoid unit (figure 14)
pu = parietal unit (figure 14)
q = quadratum (figure 14,21)
sus = suspensorium (figure 15, 22, 23)
sym = symplecticum (figure 14)
t = tibial distance between points of attach of cruciate ligaments (figure 20)
tfds = tendon of flexor digitorum superficialis (figure 14)
tpt = tendon of peroneus tertius (figure 14)
tg = tendon of gastrocnemius (figure 14)
ttc = tendon of tibialis cranialis (figure 14)
tib = tibia (figure 14)
u = urohyal (bar) (figure 18, 19)

APPENDIX 3

Table 5. *Overview of 1-, 2- and 3- parameter linkages and their transitions*

(The varied column in a 3-parameter series is boxed. Grashof- and Type-codes are listed in tables 1, 2 and 3. Some characteristic transmission functions are shown in figures 4, 5, 6, 7, 9 and 10. *a*, *b*, *c*, *d* = bar lengths; *s* = shortest bar(s), *l* = longest bar(s). *s*/*l* = short-long-ratio. c = crank (revolving bar), r = rocker (oscillating bar), cc = double-crank linkage, cr = crank-rocker linkage, rc = rocker-crank linkage, rr = double-rocker linkage. Crank-rocker transitions in a 3-parameter series are indicated in a variation direction from short to long bar lengths. The first transition which is met is indicated in the Table. For example, in 3Pslsl(1), the first crank-rocker transition occurs between a linkage with approximate dimensions: 8.8 11.0 9.0 11.0 (cr, not indicated) and the linkage: 9.0 11.0 9.0 11.0 (cc, indicated in the table). The second crank-rocker transition (between: 9.0 11.0 9.0 11.0 (cc) and: 9.2 11.0 9.0 11.0 (rc)) is fully indicated in the table. Otherwise, it would not be clear where this transition would occur exactly. Examples of crank-rocker transitions are also drawn in figure 13*b*. The linkages containing a bar length of 3.0 were chosen as examples of linkages possessing a very short link. In fact, this link may vary between zero and the first transitional bar length.)

col. 1	2	3	4	5	6	7	8	9
a	*b*	*c*	*d*	perimeter	*s/l*	Grashof	c-r	type
1R								
10.0	10.0	10.0	10.0	40.0	1.000	rhombus	cc	rhombus
2P								
9.0	11.0	9.0	11.0	40.0	0.818	4A par	cc	2Pslsl
11.0	9.0	11.0	9.0	40.0	0.818	4A par	cc	2Pslsl
3Pslsl(1)								
3.0	11.0	9.0	11.0	34.0	0.273	1A	cr	
9.0	11.0	9.0	11.0	40.0	0.818	4A par	cc	2Pslsl
9.2	11.0	9.0	11.0	40.2	0.818	1B	rc	
11.0	11.0	9.0	11.0	42.0	0.818	1B	rc	2T3s
13.0	11.0	9.0	11.0	44.0	0.692	3B	rc	3Sopp(lmsm)
13.2	11.0	9.0	11.0	44.2	0.682	2	rr	
3Pslsl(2)								
9.0	3.0	9.0	11.0	32.0	0.273	1C	cc	
9.0	7.0	9.0	11.0	36.0	0.636	3C	cc	3Sopp(msml)
9.0	7.2	9.0	11.0	36.2	0.653	2	rr	
9.0	9.0	9.0	11.0	38.0	0.818	2	rr	2T4l
9.0	11.0	9.0	11.0	40.0	0.818	4A par	cc	2Pslsl
9.0	11.2	9.0	11.0	40.2	0.804	2	rr	
3Pslsl(3)								
9.0	11.0	3.0	11.0	34.0	0.273	1B	rc	
9.0	11.0	9.0	11.0	40.0	0.818	4A par	cc	2Pslsl
9.0	11.0	9.2	11.0	40.2	0.818	1A	cr	
9.0	11.0	11.0	11.0	42.0	0.818	1A	cr	2T1s
9.0	11.0	13.0	11.0	44.0	0.692	3A	cr	3Sopp(smlm)
9.0	11.0	13.2	11.0	44.2	0.682	2	rr	
3Pslsl(4)								
9.0	11.0	9.0	3.0	32.0	0.273	1D	rr	
9.0	11.0	9.0	7.0	36.0	0.636	3D	rr	3Sopp(mlms)
9.0	11.0	9.0	9.0	38.0	0.818	2	rr	2T2l
9.0	11.0	9.0	11.0	40.0	0.818	4A par	cc	2Pslsl
9.0	11.0	9.0	11.2	40.2	0.804	2	rr	
3Plsls(1)								
3.0	9.0	11.0	9.0	32.0	0.273	1A	cr	
7.0	9.0	11.0	9.0	36.0	0.636	3A	cr	3Sopp(smlm)
7.2	9.0	11.0	9.0	36.2	0.653	2	rr	
9.0	9.0	11.0	9.0	38.0	0.818	2	rr	2T3l
11.0	9.0	11.0	9.0	40.0	0.818	4A par	cc	2Plsls
11.2	9.0	11.0	9.0	40.2	0.804	2	rr	
3Plsls(2)								
11.0	3.0	11.0	9.0	34.0	0.273	1C	cc	
11.0	9.0	11.0	9.0	40.0	0.818	4A par	cc	2Plsls
11.0	9.2	11.0	9.0	40.2	0.818	1D	rr	
11.0	11.0	11.0	9.0	42.0	0.818	1D	rr	2T4s
11.0	13.0	11.0	9.0	44.0	0.692	3D	rr	3Sopp(mlms)
3Plsls(3)								
11.0	9.0	3.0	9.0	32.0	0.273	1B	rc	
11.0	9.0	7.0	9.0	36.0	0.636	3B	rc	3Sopp(lmsm)
11.0	9.0	7.2	9.0	36.2	0.653	2	rr	
11.0	9.0	9.0	9.0	38.0	0.818	2	rr	2T1l
11.0	9.0	11.0	9.0	40.0	0.818	4A par	cc	2Plsls
11.0	9.0	11.2	9.0	40.2	0.804	2	rr	
3Plsls(4)								
11.0	9.0	11.0	3.0	34.0	0.273	1D	rr	
11.0	9.0	11.0	9.0	40.0	0.818	4A par	cc	2Plsls
11.0	9.0	11.0	11.0	42.0	0.818	1C	cc	2T2s
11.0	9.0	11.0	13.0	44.0	0.692	3C	cc	3Sopp(msml)
11.0	9.0	11.0	13.2	44.2	0.682	2	rr	

col. 1	2	3	4	5	6	7	8	9
a	*b*	*c*	*d*	perimeter	*s/l*	Grashof	c-r	type
2K								
9.0	9.0	11.0	11.0	40.0	0.818	4B kite	cc	2Kssll
11.0	11.0	9.0	9.0	40.0	0.818	4C kite	rc	2Kllss
9.0	11.0	11.0	9.0	40.0	0.818	4C kite	cr	2Kslls
11.0	9.0	9.0	11.0	40.0	0.818	4B kite	cc	2Klssl
3Kssll(1)								
3.0	9.0	11.0	11.0	34.0	0.273	1A	cr	
9.0	9.0	11.0	11.0	40.0	0.818	4B kite	cc	2Kssll
11.0	9.0	11.0	11.0	42.0	0.818	1C	cc	2T2s
13.0	9.0	11.0	11.0	44.0	0.692	3C	cc	3Sadj(lsmm)
13.2	9.0	11.0	11.0	44.2	0.682	2	rr	
3Kssll(2)								
9.0	3.0	11.0	11.0	34.0	0.273	1C	cc	
9.0	9.0	11.0	11.0	40.0	0.818	4B kite	cc	2Kssll
9.0	9.2	11.0	11.0	40.2	0.818	1A	cr	
9.0	11.0	11.0	11.0	42.0	0.818	1A	cr	2T1s
9.0	13.0	11.0	11.0	44.0	0.692	3A	cr	3Sadj(slmm)
9.0	13.2	11.0	11.0	44.2	0.682	2	rr	
3Kssll(3)								
9.0	9.0	3.0	11.0	32.0	0.273	1B	rc	
9.0	9.0	7.0	11.0	36.0	0.636	3B	rc	3Sadj(mmsl)
9.0	9.0	7.2	11.0	36.2	0.653	2	rr	
9.0	9.0	9.0	11.0	38.0	0.818	2	rr	2T4l
9.0	9.0	11.0	11.0	40.0	0.818	4B kite	cc	2Kssll
9.0	9.0	11.2	11.0	40.2	0.804	2	rr	
3Kssll(4)								
9.0	9.0	11.0	3.0	32.0	0.273	1D	rr	
9.0	9.0	11.0	7.0	36.0	0.636	3D	rr	3Sadj(mmls)
9.0	9.0	11.0	9.0	38.0	0.818	2	rr	2T3l
9.0	9.0	11.0	11.0	40.0	0.818	4B kite	cc	2Kssll
9.0	9.0	11.0	11.2	40.2	0.804	2	rr	
3Kllss(1)								
3.0	11.0	9.0	9.0	32.0	0.273	1A	cr	
7.0	11.0	9.0	9.0	36.0	0.636	3A	cr	3Sadj(slmm)
7.2	11.0	9.0	9.0	36.2	0.653	2	rr	
9.0	11.0	9.0	9.0	38.0	0.818	2	rr	2T2l
11.0	11.0	9.0	9.0	40.0	0.818	4C kite	rc	2Kllss
11.2	11.0	9.0	9.0	40.2	0.804	2	rr	
3Kllss(2)								
11.0	3.0	9.0	9.0	32.0	0.273	1C	cc	
11.0	7.0	9.0	9.0	36.0	0.636	3C	cc	3Sadj(lsmm)
11.0	7.2	9.0	9.0	36.2	0.653	2	rr	
11.0	9.0	9.0	9.0	38.0	0.818	2	rr	2T1l
11.0	11.0	9.0	9.0	40.0	0.818	4C kite	rc	2Kllss
11.0	11.2	9.0	9.0	40.2	0.804	2	rr	
3Kllss(3)								
11.0	11.0	3.0	9.0	34.0	0.273	1B	rc	
11.0	11.0	9.0	9.0	40.0	0.818	4C kite	rc	2Kllss
11.0	11.0	9.2	9.0	40.2	0.818	1D	rr	
11.0	11.0	11.0	9.0	42.0	0.818	1D	rr	2T4s
11.0	11.0	13.0	9.0	44.0	0.692	3D	rr	3Sadj(mmls)
3Kllss(4)								
11.0	11.0	9.0	3.0	34.0	0.273	1D	rr	
11.0	11.0	9.0	9.0	40.0	0.818	4C kite	rc	2Kllss
11.0	11.0	9.0	11.0	42.0	0.818	1B	rc	2T3s
11.0	11.0	9.0	13.0	44.0	0.692	3B	rc	3Sadj(mmsl)
11.0	11.0	9.0	13.2	44.2	0.682	2	rr	

col. 1	2	3	4	5	6	7	8	9
a	*b*	*c*	*d*	perimeter	*s/l*	Grashof	c-r	type
3Kslls(1)								
3.0	11.0	11.0	9.0	34.0	0.273	1A	cr	
9.0	11.0	11.0	9.0	40.0	0.818	4C kite	cr	2Kslls
9.2	11.0	11.0	9.0	40.2	0.818	1D	rr	
11.0	11.0	11.0	9.0	42.0	0.818	1D	rr	2T4s
13.0	11.0	11.0	9.0	44.0	0.692	3D	rr	3Sadj(lmms)
3Kslls(2)								
9.0	3.0	11.0	9.0	32.0	0.273	1C	cc	
9.0	7.0	11.0	9.0	36.0	0.636	3C	cc	3Sadj(mslm)
9.0	7.2	11.0	9.0	36.2	0.653	2	rr	
9.0	9.0	11.0	9.0	38.0	0.818	2	rr	2T3l
9.0	11.0	11.0	9.0	40.0	0.818	4C kite	cr	2Kslls
9.0	11.2	11.0	9.0	40.2	0.804	2	rr	
3Kslls(3)								
9.0	11.0	3.0	9.0	32.0	0.273	1B	rc	
9.0	11.0	7.0	9.0	36.0	0.636	3B	rc	3Sadj(mlsm)
9.0	11.0	7.2	9.0	36.2	0.653	2	rr	
9.0	11.0	9.0	9.0	38.0	0.818	2	rr	2T2l
9.0	11.0	11.0	9.0	40.0	0.818	4C kite	cr	2Kslls
9.0	11.0	11.2	9.0	40.2	0.804	2	rr	
3Kslls(4)								
9.0	11.0	11.0	3.0	34.0	0.273	1D	rr	
9.0	11.0	11.0	9.0	40.0	0.818	4C kite	cr	2Kslls
9.0	11.0	11.0	11.0	42.0	0.818	1A	cr	2T1s
9.0	11.0	11.0	13.0	44.0	0.692	3A	cr	3Sadj(smml)
9.0	11.0	11.0	13.2	44.2	0.682	2	rr	
3Klssl(1)								
3.0	9.0	9.0	11.0	32.0	0.273	1A	cr	
7.0	9.0	9.0	11.0	36.0	0.636	3A	cr	3Sadj(smml)
7.2	9.0	9.0	11.0	36.2	0.653	2	rr	
9.0	9.0	9.0	11.0	38.0	0.818	2	rr	2T4l
11.0	9.0	9.0	11.0	40.0	0.818	4B kite	cc	2Klssl
11.2	9.0	9.0	11.0	40.2	0.804	2	rr	
3Klssl(2)								
11.0	3.0	9.0	11.0	34.0	0.273	1C	cc	
11.0	9.0	9.0	11.0	40.0	0.818	4B kite	cc	2Klssl
11.0	9.2	9.0	11.0	40.2	0.818	1B	rc	
11.0	11.0	9.0	11.0	42.0	0.818	1B	rc	2T3s
11.0	13.0	9.0	11.0	44.0	0.692	3B	rc	3Sadj(mlsm)
11.0	13.2	9.0	11.0	44.2	0.682	2	rr	
3Klssl(3)								
11.0	9.0	3.0	11.0	34.0	0.273	1B	rc	
11.0	9.0	9.0	11.0	40.0	0.818	4B kite	cc	2Klssl
11.0	9.0	11.0	11.0	42.0	0.818	1C	cc	2T2s
11.0	9.0	13.0	11.0	44.0	0.692	3C	cc	3Sadj(mslm)
11.0	9.0	13.2	11.0	44.2	0.682	2	rr	
3Klssl(4)								
11.0	9.0	9.0	3.0	32.0	0.273	1D	rr	
11.0	9.0	9.0	7.0	36.0	0.636	3D	rr	3Sadj(lmms)
11.0	9.0	9.0	9.0	38.0	0.818	2	rr	2T1l
11.0	9.0	9.0	11.0	40.0	0.818	4B kite	cc	2Klssl
11.0	9.0	9.0	11.2	40.2	0.804	2	rr	

col. 1	2	3	4	5	6	7	8	9
a	*b*	*c*	*d*	perimeter	*s/l*	Grashof	c-r	type
2T1								
11.0	9.0	9.0	9.0	38.0	0.818	2	rr	2T1l
9.0	11.0	11.0	11.0	42.0	0.818	1A	cr	2T1s
3T1l(1) and 3T1s(1)								
3.0	9.0	9.0	9.0	30.0	0.333	1A	cr	2T1s
9.0	9.0	9.0	9.0	36.0	1.000	rhombus	cc	rhombus
9.1	9.0	9.0	9.0	36.1	0.990	2	rr	2T1l
3T1l(2)								
11.0	3.0	9.0	9.0	32.0	0.273	1C	cc	
11.0	7.0	9.0	9.0	36.0	0.636	3C	cc	3Sadj(lsmm)
11.0	7.2	9.0	9.0	36.2	0.653	2	rr	
11.0	9.0	9.0	9.0	38.0	0.818	2	rr	2T1l
11.0	11.0	9.0	9.0	40.0	0.818	4C kite	rc	2Kllss
11.0	11.2	9.0	9.0	40.2	0.804	2	rr	
3T1s(2)								
9.0	3.0	11.0	11.0	34.0	0.273	1C	cc	
9.0	9.0	11.0	11.0	40.0	0.818	4B kite	cc	2Kssll
9.0	9.2	11.0	11.0	40.2	0.818	1A	cr	
9.0	11.0	11.0	11.0	42.0	0.818	1A	cr	2T1s
9.0	13.0	11.0	11.0	44.0	0.692	3A	cr	3Sadj(slmm)
9.0	13.2	11.0	11.0	44.2	0.682	2	rr	
3T1l(3)								
11.0	9.0	3.0	9.0	32.0	0.273	1B	rc	
11.0	9.0	7.0	9.0	36.0	0.636	3B	rc	3Sopp(lmsm)
11.0	9.0	7.2	9.0	36.2	0.653	2	rr	
11.0	9.0	9.0	9.0	38.0	0.818	2	rr	2T1l
11.0	9.0	11.0	9.0	40.0	0.818	4A par	cc	2Plsls
11.0	9.0	11.2	9.0	40.2	0.804	2	rr	
3T1s(3)								
9.0	11.0	3.0	11.0	34.0	0.273	1B	rc	
9.0	11.0	9.0	11.0	40.0	0.818	4A par	cc	2Pslsl
9.0	11.0	9.2	11.0	40.2	0.818	1A	cr	
9.0	11.0	11.0	11.0	42.0	0.818	1A	cr	2T1s
9.0	11.0	13.0	11.0	44.0	0.692	3A	cr	3Sopp(smlm)
9.0	11.0	13.2	11.0	44.2	0.682	2	rr	
3T1l(4)								
11.0	9.0	9.0	3.0	32.0	0.273	1D	rr	
11.0	9.0	9.0	7.0	36.0	0.636	3D	rr	3Sadj(lmms)
11.0	9.0	9.0	9.0	38.0	0.818	2	rr	2T1l
11.0	9.0	9.0	11.0	40.0	0.818	4B kite	cc	2Klssl
11.0	9.0	9.0	11.2	40.2	0.804	2	rr	
3T1s(4)								
9.0	11.0	11.0	3.0	34.0	0.273	1D	rr	
9.0	11.0	11.0	9.0	40.0	0.818	4C kite	cr	2Kslls
9.0	11.0	11.0	11.0	42.0	0.818	1A	cr	2T1s
9.0	11.0	11.0	13.0	44.0	0.692	3A	cr	3Sadj(smml)
9.0	11.0	11.0	13.2	44.2	0.682	2	rr	

col. 1	2	3	4	5	6	7	8	9
a	*b*	*c*	*d*	perimeter	*s/l*	Grashof	c-r	type
2T2								
9.0	11.0	9.0	9.0	38.0	0.818	2	rr	2T2l
11.0	9.0	11.0	11.0	42.0	0.818	1C	cc	2T2s
3T2l(1)								
3.0	11.0	9.0	9.0	32.0	0.273	1A	cr	
7.0	11.0	9.0	9.0	36.0	0.636	3A	cr	3Sadj(slmm)
7.2	11.0	9.0	9.0	36.2	0.653	2	rr	
9.0	11.0	9.0	9.0	38.0	0.818	2	rr	2T2l
11.0	11.0	9.0	9.0	40.0	0.818	4C kite	rc	2Kllss
11.2	11.0	9.0	9.0	40.2	0.804	2	rr	
3T2s(1)								
3.0	9.0	11.0	11.0	34.0	0.273	1A	cr	
9.0	9.0	11.0	11.0	40.0	0.818	4B kite	cc	2Kssll
11.0	9.0	11.0	11.0	42.0	0.818	1C	cc	2T2s
13.0	9.0	11.0	11.0	44.0	0.692	3C	cc	3Sadj(lsmm)
13.2	9.0	11.0	11.0	44.2	0.682	2	rr	
3T2l(2) and 3T2s(2)								
9.0	3.0	9.0	9.0	30.0	0.333	1C	cc	2T2s
9.0	9.0	9.0	9.0	36.0	1.000	rhombus	cc	rhombus
9.0	9.1	9.0	9.0	36.1	0.990	2	rr	2T2l
3T2l(3)								
9.0	11.0	3.0	9.0	32.0	0.273	1B	rc	
9.0	11.0	7.0	9.0	36.0	0.636	3B	rc	3Sadj(mlsm)
9.0	11.0	7.2	9.0	36.2	0.653	2	rr	
9.0	11.0	9.0	9.0	38.0	0.818	2	rr	2T2l
9.0	11.0	11.0	9.0	40.0	0.818	4C kite	cr	2Kslls
9.0	11.0	11.2	9.0	40.2	0.804	2	rr	
3T2s(3)								
11.0	9.0	3.0	11.0	34.0	0.273	1B	rc	
11.0	9.0	9.0	11.0	40.0	0.818	4B kite	cc	2Klssl
11.0	9.0	11.0	11.0	42.0	0.818	1C	cc	2T2s
11.0	9.0	13.0	11.0	44.0	0.692	3C	cc	3Sadj(mslm)
11.0	9.0	13.2	11.0	44.2	0.682	2	rr	
3T2l(4)								
9.0	11.0	9.0	3.0	32.0	0.273	1D	rr	
9.0	11.0	9.0	7.0	36.0	0.636	3D	rr	3Sopp(mlms)
9.0	11.0	9.0	9.0	38.0	0.818	2	rr	2T2l
9.0	11.0	9.0	11.0	40.0	0.818	4A par	cc	2Pslsl
9.0	11.0	9.0	11.2	40.2	0.804	2	rr	
3T2s(4)								
11.0	9.0	11.0	3.0	34.0	0.273	1D	rr	
11.0	9.0	11.0	9.0	40.0	0.818	4A par	cc	2Plsls
11.0	9.0	11.0	11.0	42.0	0.818	1C	cc	2T2s
11.0	9.0	11.0	13.0	44.0	0.692	3C	cc	3Sopp(msml)
11.0	9.0	11.0	13.2	44.2	0.682	2	rr	

col. 1	2	3	4	5	6	7	8	9
a	*b*	*c*	*d*	perimeter	*s/l*	Grashof	c-r	type
2T3								
9.0	9.0	11.0	9.0	38.0	0.818	2	rr	2T3l
11.0	11.0	9.0	11.0	42.0	0.818	1B	rc	2T3s
3T3l(1)								
3.0	9.0	11.0	9.0	32.0	0.273	1A	cr	
7.0	9.0	11.0	9.0	36.0	0.636	3A	cr	3Sopp(smlm)
7.2	9.0	11.0	9.0	36.2	0.653	2	rr	
9.0	9.0	11.0	9.0	38.0	0.818	2	rr	2T3l
11.0	9.0	11.0	9.0	40.0	0.818	4A par	cc	2Plsls
11.2	9.0	11.0	9.0	40.2	0.804	2	rr	
3T3s(1)								
3.0	11.0	9.0	11.0	34.0	0.273	1A	cr	
9.0	11.0	9.0	11.0	40.0	0.818	4A par	cc	2Pslsl
9.2	11.0	9.0	11.0	40.2	0.818	1B	rc	
11.0	11.0	9.0	11.0	42.0	0.818	1B	rc	2T3s
13.0	11.0	9.0	11.0	44.0	0.692	3B	rc	3Sopp(lmsm)
13.2	11.0	9.0	11.0	44.2	0.682	2	rr	
3T3l(2)								
9.0	3.0	11.0	9.0	32.0	0.273	1C	cc	
9.0	7.0	11.0	9.0	36.0	0.636	3C	cc	3Sadj(mslm)
9.0	7.2	11.0	9.0	36.2	0.653	2	rr	
9.0	9.0	11.0	9.0	38.0	0.818	2	rr	2T3l
9.0	11.0	11.0	9.0	40.0	0.818	4C kite	cr	2Kslls
9.0	11.2	11.0	9.0	40.2	0.804	2	rr	
3T3s(2)								
11.0	3.0	9.0	11.0	34.0	0.273	1C	cc	
11.0	9.0	9.0	11.0	40.0	0.818	4B kite	cc	2Klssl
11.0	9.2	9.0	11.0	40.2	0.818	1B	rc	
11.0	11.0	9.0	11.0	42.0	0.818	1B	rc	2T3s
11.0	13.0	9.0	11.0	44.0	0.692	3B	rc	3Sadj(mlsm)
11.0	13.2	9.0	11.0	44.2	0.682	2	rr	
3T3l(3) and 3T3s(3)								
9.0	9.0	3.0	9.0	30.0	0.333	1B	rc	2T3s
9.0	9.0	9.0	9.0	36.0	1.000	rhombus	cc	rhombus
9.0	9.0	9.1	9.0	36.1	0.990	2	rr	2T3l
3T3l(4)								
9.0	9.0	11.0	3.0	32.0	0.273	1D	rr	
9.0	9.0	11.0	7.0	36.0	0.636	3D	rr	3Sadj(mmls)
9.0	9.0	11.0	9.0	38.0	0.818	2	rr	2T3l
9.0	9.0	11.0	11.0	40.0	0.818	4B kite	cc	2Kssll
9.0	9.0	11.0	11.2	40.2	0.804	2	rr	
3T3s(4)								
11.0	11.0	9.0	3.0	34.0	0.273	1D	rr	
11.0	11.0	9.0	9.0	40.0	0.818	4C kite	rc	2Kllss
11.0	11.0	9.0	11.0	42.0	0.818	1B	rc	2T3s
11.0	11.0	9.0	13.0	44.0	0.692	3B	rc	3Sadj(mmsl)
11.0	11.0	9.0	13.2	44.2	0.682	2	rr	

col. 1	2	3	4	5	6	7	8	9
a	*b*	*c*	*d*	perimeter	*s/l*	Grashof	c-r	type
2T4								
9.0	9.0	9.0	11.0	38.0	0.818	2	rr	2T4l
11.0	11.0	11.0	9.0	42.0	0.818	1D	rr	2T4s
3T4l(1)								
3.0	9.0	9.0	11.0	32.0	0.273	1A	cr	
7.0	9.0	9.0	11.0	36.0	0.636	3A	cr	3Sadj(smml)
7.2	9.0	9.0	11.0	36.2	0.653	2	rr	
9.0	9.0	9.0	11.0	38.0	0.818	2	rr	2T4l
11.0	9.0	9.0	11.0	40.0	0.818	4B kite	cc	2Klssl
11.2	9.0	9.0	11.0	40.2	0.804	2	rr	
3T4s(1)								
3.0	11.0	11.0	9.0	34.0	0.273	1A	cr	
9.0	11.0	11.0	9.0	40.0	0.818	4C kite	cr	2Kslls
9.2	11.0	11.0	9.0	40.2	0.818	1D	rr	
11.0	11.0	11.0	9.0	42.0	0.818	1D	rr	2T4s
13.0	11.0	11.0	9.0	44.0	0.692	3D	rr	3Sadj(lmms)
3T4l(2)								
9.0	3.0	9.0	11.0	32.0	0.273	1C	cc	
9.0	7.0	9.0	11.0	36.0	0.636	3C	cc	3Sopp(msml)
9.0	7.2	9.0	11.0	36.2	0.653	2	rr	
9.0	9.0	9.0	11.0	38.0	0.818	2	rr	2T4l
9.0	11.0	9.0	11.0	40.0	0.818	4A par	cc	2Pslsl
9.0	11.2	9.0	11.0	40.2	0.804	2	rr	
3T4s(2)								
11.0	3.0	11.0	9.0	34.0	0.273	1C	cc	
11.0	9.0	11.0	9.0	40.0	0.818	4A par	cc	2Plsls
11.0	9.2	11.0	9.0	40.2	0.818	1D	rr	
11.0	11.0	11.0	9.0	42.0	0.818	1D	rr	2T4s
11.0	13.0	11.0	9.0	44.0	0.692	3D	rr	3Sopp(mlms)

col. 1	2	3	4	5	6	7	8	9
a	*b*	*c*	*d*	perimeter	*s/l*	Grashof	c-r	type
3T4l(3)								
9.0	9.0	3.0	11.0	32.0	0.273	1B	rc	
9.0	9.0	7.0	11.0	36.0	0.636	3B	rc	3Sadj(mmsl)
9.0	9.0	7.2	11.0	36.2	0.653	2	rr	
9.0	9.0	9.0	11.0	38.0	0.818	2	rr	2T4l
9.0	9.0	11.0	11.0	40.0	0.818	4B kite	cc	2Kssll
9.0	9.0	11.2	11.0	40.2	0.804	2	rr	
3T4s(3)								
11.0	11.0	3.0	9.0	34.0	0.273	1B	rc	
11.0	11.0	9.0	9.0	40.0	0.818	4C kite	rc	2Kllss
11.0	11.0	9.2	9.0	40.2	0.818	1D	rr	
11.0	11.0	11.0	9.0	42.0	0.818	1D	rr	2T4s
11.0	11.0	13.0	9.0	44.0	0.692	3D	rr	3Sadj(mmls)
3T4l(4) and 3T4s(4)								
9.0	9.0	9.0	3.0	30.0	0.333	1D	rr	2T4s
9.0	9.0	9.0	9.0	36.0	1.000	rhombus	cc	rhombus
9.0	9.0	9.0	9.1	36.1	0.990	2	rr	2T4l